(12)

HIGH-LIFT CAPABILITY OF LOW ASPECT RATIO WINGS UTILIZING CIRCULATION CONTROL AND UPPER SURFACE BLOWING

by

Roger J. Furey

AVIATION AND SURFACE EFFECTS DEPARTMENT

DTNSRDC/ASED-80/15

July 1980

DAVID W. TAYLOR NAVAL SHIP RESEARCH AND DEVELOPMENT CENTER
BETHESDA
MARYLAND
20084

UNCLASSIFIED

SECURITY CLASSIFICATION OF THIS PAGE (When Data Entered)

REPORT DOCUMENTATION PAGE	READ INSTRUCTIONS BEFORE COMPLETING FORM
1. REPORT NUMBER: DTNSRDC/ASED-80/15	2. GOVT ACCESSION NO.: AD-A112 343
	3. RECIPIENT'S CATALOG NUMBER:
4. TITLE (and Subtitle): HIGH LIFT CAPABILITY OF LOW ASPECT RATIO WINGS UTILIZING CIRCULATION CONTROL AND UPPER SURFACE BLOWING	5. TYPE OF REPORT & PERIOD COVERED: Interim
	6. PERFORMING ORG. REPORT NUMBER:
7. AUTHOR(s): Roger J. Furey	8. CONTRACT OR GRANT NUMBER(s):
9. PERFORMING ORGANIZATION NAME AND ADDRESS: David Taylor Naval Ship Research and Development Center, Bethesda, Maryland 20084	10. PROGRAM ELEMENT, PROJECT, TASK AREA & WORK UNIT NUMBERS: Task Area WF41 421 000, Program Element 6224111, Work Unit 1-1660-079
11. CONTROLLING OFFICE NAME AND ADDRESS: Naval Air Systems Command, AIR 320D, Washington, D.C.	12. REPORT DATE: July 1980
	13. NUMBER OF PAGES: 73
14. MONITORING AGENCY NAME & ADDRESS(if different from Controlling Office)	15. SECURITY CLASS. (of this report): UNCLASSIFIED
	15a. DECLASSIFICATION/DOWNGRADING SCHEDULE

16. DISTRIBUTION STATEMENT (of this Report)

APPROVED FOR PUBLIC RELEASE: DISTRIBUTION UNLIMITED

17. DISTRIBUTION STATEMENT (of the abstract entered in Block 20, if different from Report)

18. SUPPLEMENTARY NOTES

19. KEY WORDS (Continue on reverse side if necessary and identify by block number)

Low Aspect Ratio Wings
Powered-Lift Systems
Lift Augmentation

20. ABSTRACT (Continue on reverse side if necessary and identify by block number)

A semispan research model with a 2-ft span wing was used to measure the high lift capabilities of low aspect ratio wings utilizing powered-lift concepts. The concepts evaluated were the Circulation Control Wing (CCW), the Upper Surface Blowing (USB), and a unique combination of the two (CCW/USB). Wing tip sails were used as a means of increasing the effective aspect ratio of these wings during high lift.

DD FORM 1 JAN 73 1473 EDITION OF 1 NOV 65 IS OBSOLETE
S/N 0102-LF-014-6601

SECURITY CLASSIFICATION OF THIS PAGE (When Data Entered)

(Block 20 continued)

The highest lift was generated with the CCW/USB configuration where the CCW is used as a thrust vectoring device and successfully turns the engine exhaust up to 165 deg. The lift augmentation resulting from the CCW and the turning exhaust flow prodiced a $C_{L_{max}}$ of 5.1 with an aspect ratio 4 wing. It is shown that this nearly approaches the theoretical maximum circulation lift (independent of the thrust contribution to lift) that can be developed for a given aspect ratio wing. The wing tip sails are effective in reducing the induced drag of these powered-lift low aspect ratio wings under high-lift conditions. The induced drag factor is reduced in some instances by 30 to 35 percent. The relatively low drag of this configuration shows that with correct operational procedure the potential for short takeoff and landing is significant.

TABLE OF CONTENTS

LIST OF FIGURES

LIST OF FIGURES

LIST OF FIGURES

NOTATION

AR	Aspect ratio, b^2/S
b	Wing span, ft (m)
C_D	Drag coefficient, D/qS
C_{D_o}	Drag coefficient at zero lift
C_L	Lift coefficient, L/qS
C_{L_α}	Lift curve slope, $\partial C_L / \partial \alpha$
$C_{L_{max}}$	Maximum lift coefficient
C_T	Thrust coefficient, T/qS
C_μ	Momentum coefficient, $\dot{m}Vj/qS$
c	Wing chord, ft (m)
D	Drag, lb (N)
e	Oswald efficiency factor
K	Induced drag factor, $1/\pi ARe$
L	Lift, lb (N)
m	Mass flow
P_{T_d}	Duct total pressure, lb/in.^{2} (N/m^2)
q	Dynamic pressure, $1/2\ \rho\ V^2$
S	Wing reference area, ft^2 (m^2)
T	Thrust, lb (m)
V	Free-stream velocity, ft/sec (m/s)
V_j	Jet velocity, ft/sec (m/s)
α	Angle of attack, deg
δ_f	Trailing edge flap angle, deg
δn	Leading edge flap angle, deg

ABSTRACT

A semispan research model with a 2-ft span wing was used to measure the high-lift capabilities of low aspect ratio wings utilizing powered-lift concepts. The concepts evaluated were the Circulation Control Wing (CCW), the Upper Surface Blowing (USB), and a unique combination of the two (CCW/USB). Wing tip sails were used as a means of increasing the effective aspect ratio of these wings during high lift.

The highest lift was generated with the CCW/USB configuration where the CCW is used as a thrust vectoring device and successfully turns the engine exhaust up to 165 deg. The lift augmentation resulting from the CCW and the turning exhaust flow produced a $C_{L_{max}}$ of 5.1 with an aspect ratio 4 wing. It is shown that this nearly approaches the theoretical maximum circulation lift (independent of the thrust contribution to lift) that can be developed for a given aspect ratio wing. The wing tip sails are effective in reducing the induced drag of these powered-lift low aspect ratio wings under high-lift conditions. The induced drag factor is reduced in some instances by 30 to 35 percent. The relatively low drag of this configuration shows that with correct operational procedure the potential for short takeoff and landing is significant.

ADMINISTRATIVE INFORMATION

The work reported was authorized by the Naval Air Systems Command (AIR 320) and was funded under WF 41 421 000, Work Unit 1660-079.

INTRODUCTION

The operating constraints of many types of naval aircraft, (that is, restricted size in landing and takeoff platforms) and the ever-increasing costs of building and supporting the current type of conventional aircraft carrier, have caused considerable interest in short takeoff and landing (STOL) aircraft as a means of reducing some of these difficulties.

The restriction of a 45-ft wing span when operating from a landing platform helicopter (LPH) size ship (which is often suggested as the nominal size for a future sea control ship) necessitates the use of a less efficient low aspect ratio wing.* In order to realize the platform restrictions, the performance of such aircraft are compromised in cruise and range. The current effort completes a low aspect ratio high-lift wing aerodynamics study at David Taylor Naval Ship Research and Development Center (DTNSRDC) to develop the means of overcoming the platform restrictions.[1]**

A number of powered-lift concepts have been studied with high aspect ratio wings as a possible means of achieving efficient STOL performance. References 2 through 6 present a number of these efforts in which the most promising concepts are evaluated. Two of these approaches are the Upper Surface Blowing (USB) and the Circulation Control Wing (CCW). Both concepts use the Coanda effect as a means of augmenting aerodynamic lift.

In the case of the USB concept, the exhaust nozzle flow of an above-the-wing mounted turbofan engine is turned a predetermined amount by a continuous surface trailing edge flap which provides the Coanda turning until separated flow on the surface occurs. In addition to the thrust component added to the lift direction, a certain amount of lift augmentation is achieved by entraining free-stream air into the exhaust flow.

The CCW concept employs a spanwise thin trailing edge slot which expels a jet of air over a rounded trailing edge. The Coanda turning of this jet relocates the

---

*Reported informally by Harris and Trobaugh ("Comparison of the Effect of the Circulation Control Wing, Upper Surface Blown Flap, and Augmented Jet Flap on the Short Takeoff and Mission Performance of a Low Aspect Ratio Patrol Aircraft," DTNSRDC TM-16-78-02 Apr 1978).

**A complete listing of references is given on page 67.

trailing edge stagnation point and also entrains free-stream air, thereby augmenting lift totally by supercirculation (there is no contribution to lift from the jet force itself).

A third and new concept, the CCW/USB, was also studied as a means of augmenting the aerodynamic lift and vectoring the engine thrust. In this approach, the above-the-wing mounted engine has its exhaust turned by the trailing edge Coanda slot and surface. The need for the larger trailing edge mechanical flap is thereby eliminated. The three concepts with the dimensions and geometry of the basic semispan model are illustrated in Figure 1.

An additional phase of the program included enhancing the aerodynamic efficiency of low aspect ratio wings through the use of wing tip devices. The present effort was limited to an evaluation of a wing tip fence and wing tip sails. The wing tip sails are a derivative of those developed by Spillman,[7] and were originally conceived as a means of alleviating induced drag on relatively high aspect ratio wings in a cruise condition. The emphasis in this phase of the program is on applying wing tip sails to low aspect ratio wings in a high lift condition in order to (1) reduce the accompanying high induced drag for takeoff, (2) modulate the high induced drag during landing approach, and (3) reduce the induced drag of the unblown wing during cruise.

MODELS, APPARATUS, AND TEST PROCEDURES

A semispan model with a 14-percent thick supercritical wing was the basis for all three configurations tested (Figure 1). Figure 2 shows the model in the USB configuration, mounted on its groundboard in the DTNSRDC 8- by 10-ft wind tunnel. The wing is equipped to handle trailing edge flap settings of 0, 40, and 60 deg. The flap surface consisted of a continuous curved section on the inboard portion of

the wing where the engine exhaust would impinge. The outboard wing section was equipped with double slotted flaps. The propulsion simulator was a 5.5-in. diameter airdriven fan with two tip-drive turbines in tandem. The exhaust nozzle had an aspect ratio 3.3 exit area, and was equipped with an insert with a 10-deg turning angle deflecting the flow toward the wing surface. Additional sections could be added to the outboard portion of the wing to create aspect ratios of 3, 4, and 5. A leading edge flap which was 15 percent of the wing chord and projected at an angle of 40 deg to the wing chord was used with the 40- and 60-deg flap settings. Transition strips of number 30 grit were placed approximately 1 in. behind the wing leading edge.

The CCW model is shown in Figure 3. In this arrangement, the forward portion of the wing is the same 14-percent thick supercritical section used in the USB configuration. The trailing edge has been modified to provide for the internal air passage, the trailing edge slot, and the rounded trailing edge that makes up the circulation control wing. Figure 3 also shows the wing tip fence used to delay tip stall on some of the configurations.

In the CCW/USB arrangement presented in Figure 4, the forward portion of the wing and the engine assembly is identical to that of the USB model. The trailing edge continuous flap section has been replaced with the CCW trailing edge. The turning of the engine exhaust (thrust vectoring) is provided by the CCW trailing edge. This configuration was investigated only in the aspect ratio 4 arrangement.

Since one of the objectives of the program was to increase the effectiveness of low aspect ratio wings, an initial and limited portion of the test included an appraisal of wing tip devices as a means of increasing the effective aspect ratio. In addition to the tip fence in Figure 3, an arrangement of "sails" was also

studied. The tip sails were a derivative of those developed at the Cranfield Institute[7] for the purpose of increasing the effective aspect ratio of a given wing. In the Cranfield studies, tip sails were shown to reduce the induced drag of the Paris aircraft by 20 percent. These sails were included in the present study to observe if this approach would be equally effective for low aspect ratio high-lift conditions.

The tests were conducted in the 8- by 10-ft north subsonic wind tunnel at DTNSRDC. This wind tunnel is of the closed circuit type and is capable of continuous operation at atmospheric pressure. Although the facility can generate dynamic pressure up to 80 lb/ft^2 (3830 N/m^2), the greater portion of this test was conducted at 20 lb/ft^2 (957 N/m^2). This provides a Reynolds Number of 0.8×10^6 per foot.

The semispan model was floor-mounted in the test section in a vertical position using a base strut system. The strut system is located beneath the tunnel floor, and transfers the aerodynamic loads of the model to an external Toledo mechanical balance system. The balance system measures six component force and moment data for recording on magnetic tape utilizing a Beckman 210 high-speed acquistion system.

The wing-fuselage model was mounted in the test section such that only the wing was attached to the balance frame. The fuselage was mounted to a boundary layer splitter plate and was independent of the balance frame, with a small gap existing between wing root and fuselage body. The forces and moments measured by the balance frame are essentially wing-alone data in the presence of a body. The gap between wing root and fuselage (Figure 3) allowed air to leak from the control room below the tunnel while the tunnel was operating. To alleviate the resulting flow interference, a root fence (Figure 4) was used to divert the leakage.

The circular boundary layer splitter plate was 8 ft (2.44 m) in diameter and served as a reflection plane for the semispan model. This plate was mounted to the tunnel floor with a gap between the groundboard and floor to separate the boundary layer; see Figure 3.

The propulsion simulator was calibrated with the model assembly on the balance frame in the wind tunnel. The house air supply provides air at the rate of 1.2 lb/sec (5.38 N/s), and 165 lb/in^2 (11.4 x 10^4 N/m^2). At this rate, the engines can be driven at 26,000 rpm, which provided a thrust coefficient range from 0 to 2.0 for the test conditions considered. The momentum coefficient for the CCW and CCW/USB portions of the program ranged from 0 to 0.6 and were determined from the expression:

$$C_\mu = \frac{\dot{m}V_j}{qS}$$

where the mass flow was measured by a venturimeter located in the air supply line. The jet exit velocity was determined assuming an isentropic expansion from the wing plenum total conditions to the free-stream static conditions.

The test procedure involved establishing tunnel and model conditions q, rpm, and C_μ and sweeping the model through small angular increments. Force and moment data were recorded at each pause from -5 deg angle of attack through the stall point.

RESULTS AND DISCUSSION

EVALUATION OF WING TIP SAILS

The main objective of the program was to evaluate the effectiveness of low aspect ratio wings, in conjunction with powered-lift devices, in developing high

lift. A means of enhancing the lifting effectiveness of low aspect ratio wings also considered was the use of a tip fence and wing tip sails. Preliminary to the 8- by 10-ft tunnel tests was a brief appraisal of one of these methods, the tip sails, through the use of a DTNSRDC smoke tunnel. A 14-percent thick, aspect ratio 4, supercritical wing was fabricated for this purpose, and is shown in Figure 5 attached to the smoke tunnel wall. Models of the tip sails developed by Spillman at Cranfield were fabricated to serve as a basis of comparison for other wing tip flow enhancing devices eventually considered.

The sails (shown in Figure 5a), in accordance with Reference 8, had a span equivalent to 41 percent of the wing tip chord. The sail root chord was 16 percent of the wing tip chord, and was highly cambered in the root section where the tip vortex would be strongest. The purpose of the Cranfield tip sails was to reduce the induced drag while the wing was at relatively low angles of attack or a cruise condition. To utilize these methods at high-lift conditions, the sail local angle of attack, orientation (roll angle about the wing tip), and chord position were varied. The number of sails were varied in an attempt to favorably affect the wing tip vortex by delaying its break-up to higher angles of attack. The tip vortex pattern for the basic wing, without sails, is shown in Figure 5b.

The sails then were positioned such that the local streamline was tangent to the sail surface at the trailing edge. This condition would allow for flow attachment on the sails for the particular wing angle of attack. Figures 5c and 5d show the wing beyond stall and with the flow favorably affected by the sails. An arrangement of four sails (the most forward mounted vertically at mid chord, the most rearward mounted horizontally, and equal angular increments between the four) was most effective in maintaining the tip flow to high angles of attack.

This four-sail arrangement was also used with the CCW and USB configuration in the 8- by 10-foot wind tunnel tests.

CIRCULATION CONTROL WING

Figures 6, 7, and 8 show the lift curves and drag polars obtained with the aspect ratio 4 CCW configuration. The maximum lift coefficient obtained for this configuration was 4.0, which was achieved with the model utilizing the family of tip sails. The use of the wing tip fence and the tip sails enhanced the performance of the CCW. The improvement shown in both C_{L_α} and $C_{L_{max}}$ while using the tip fence or sails is attributed to the delay in the tip stall brought about by these devices. The tip sails proved to be somewhat more effective. In comparing common values of C_μ in Figures 7 and 8, the sails show a higher value of $C_{L_{max}}$ and delay the stall to a higher angle of attack. The drag polars of Figures 6, 7, and 8 show the tip sails have little impact on the zero or low-lift drag, but these sails definitely influence the induced drag that is developed. The induced drag is reduced over that of the plain tip configuration in both cases.

A comparison of the induced drag factor K is presented in Figure 9. The induced drag factor of the CCW with the tip sails for two representative values of C_μ shows a reduction of 30 to 35 percent over that of the plain wing tip, and this benefit is maintained into the high-lift region of interest. The pitching moments obtained from the CCW model were obtained for wing alone (measured about the 1/4-chord position). The large nose-down pitching moment typical of these powered lift configurations was apparent. The pitching moments were considerably more affected by increases in the blowing coefficient than by angle-of-attack changes. The pitching moments were also affected by the tip fence and sails. For similar values of C_μ the fence and sails produced the larger nose-down moments.

UPPER SURFACE BLOWING

Figure 10 shows various configurations of the USB model. A series of bench testing was conducted on the USB model before entering the tunnel. Initial operation of the engine nozzle combination showed the exhaust flow did not adhere to the trailing edge flap for the full extent of turning, but separated after a small degree of turning. To alleviate this, an angled insert was placed in the nozzle to deflect the flow more directly to the flap surface. The insert is shown in Figure 10a, and the resulting attached flow, in the form of oil flow, is shown in Figure 10b. The oil flow also served to determine the spanwise extent of the flap to which the exhaust would adhere. Outboard of this region, the double-slotted flaps were exposed as shown in Figure 10c.

The lift and drag characteristics of the USB model with a 40-deg flap deflection are shown in Figures 11 and 12. The data were obtained with the aspect ratio 4 wing, and employed either the wing tip fence or the four tip sails. In both instances, a $C_{L_{max}}$ of 4.8 was achieved, with the tip sails showing a slight improvement in the induced drag over that of the tip fence. The data of Figures 11 and 12 are the measured drag and, therefore, include the thrust component. This is the case with all the USB and CCW/USB configurations. The nose-down pitching moments of this configuration are slightly more severe than was the case with CCW and are less affected by angle-of-attack changes.

Figure 13 shows a make-up of the lift contribution for this configuration. The lower lift curve for each pair of curves shows the aerodynamic lift and includes whatever augmentation is attained due to increased circulation resulting from the exhaust flow being turned by the trailing edge flap. The difference between the lower lift curve and the upper curve then represents the thrust component for that

particular power setting. The figure shows that the increment in lift augmentation being attained by induced circulation due to thrust is decreasing as the thrust is increasing; that is, the thrust contribution to the lift continues to increase in proportion to the thrust, while the lift due to increased circulation may be approaching a limit. The theoretical upper limit of lift due to circulation[9] as a function of aspect ratio and values from the current program are shown in Figure 14. With the thrust component removed from the USB data, the CCW more nearly approaches the theoretical limit. The full range of the propulsion simulator was not usable in this test program due to limitations in the house air supply; however, the data of Figure 13 show the increment in circulation lift to be decreasing with increasing thrust.

Figures 15 through 17 provide the longitudinal characteristics for the USB model with a 60-deg flap deflection. The three arrangements evaluated were the plain wing tip, tip sails, and tip fence. The maximum lift coefficient of 4.7 was attained using the tip sails.

Oil flow studies of the three configurations are shown in Figure 18. The model is at an angle of attack of 18 deg. The significant portion of the flow is that about the wing tip. Figure 18a shows the plain wing tip with the flow separating about half-way down the trailing-edge 60-deg flap section. The tip fence of Figure 18b has the flow separating just behind the slotted section of the flap. Figure 18c shows the tip sails with the flow almost completely attached on the outboard flap section. This favorable effect is reflected in the lift that was generated and the drag characteristics shown in Figures 15 through 17.

The associated induced drag factors of the plain tip and the tip sails configurations are shown in Figure 19. Note that the thrust contribution has been removed. The figure also shows the induced drag associated with this model while

using no flaps. Of significance is that the difference in induced drag is more favorable for the high-lift condition with a 60-deg flap setting than it is for the no-flap or cruise condition.

The contribution to lift due to circulation and thrust for the USB model with a 60-deg flap deflection is shown in Figure 20. The limiting effect of lift augmentation because of increased circulation is apparent with little augmentation being attained beyond a thrust coefficient of 1.01. The maximum value of circulation lift obtained with this configuration is 3.3, which is equivalent to the lift obtained with the USB model and a 40-deg flap deflection, and falls right on the value shown in Figure 14.

The USB aspect ratio 4 and 0-deg flap deflection data are shown in Figures 21 through 23. In this configuration, the 14 percent thick supercritical wing is without the leading edge flap. The maximum lift coefficient is obtained with the plain wing tip. The induced drag, however, benefits with the addition of the tip sails. For comparison, the model was equipped with a wing tip extension which increased the aspect ratio to 5. The lift and drag characteristics for this configuration are provided in Figure 24. The induced drag factors for the "USB, AR = 4" with and without tip sails and the "USB, AR = 5" with plain wing tip are shown in Figure 25. The tip sails again show an improvement in the induced drag factor over that for the plain wing with the same aspect ratio. The induced drag factor for the aspect ratio 4 wing is equivalent to the plain tip for the aspect ratio 5 wing. However, extrapolating the straight lines of Figure 25 back to zero lift gives the zero lift drag which shows the penalty for using the sails. The effective aspect ratio of the wing is increased at the expense of increased drag at other than the design range of the particular sails.

CIRCULATION CONTROL WING/UPPER SURFACE BLOWING

Figures 26 through 28 show the longitudinal aerodynamic characteristics of the aspect ratio 4 CCW/USB configuration. The maximum lift coefficient of 5.1 was obtained at the maximum attainable thrust coefficient, but at a moderate level of C_μ = 0.322 (Figure 28). The effectiveness of the tip fence and sails was not measured on this configuration, therefore, all of the data pertain only to the plain wing tip.

In comparing the CCW model with similar C_μ values of 0.29 with and without tip sail (Figures 3 and 6), the maximum C_L is shown to increase from 3.3 to 3.7 when employing the sails. On this basis, the CCW/USB configuration would generate a $C_{L_{max}}$ on the order of 5.6 if sails are used. The drag polars of Figures 26 through 28 show a unique feature of the CCW/USB. At a given thrust level, an increase in the momentum coefficient C_μ causes the drag to increase as the thrust is deflected more and more, due to the trailing edge blowing. The versatility of this feature makes possible the use of this concept in reversing thrust and in vertical or hovering flight. To isolate the circulation lift on the CCW/USB configuration, it is necessary to determine the degree of thrust vectoring that is achieved with various levels of C_μ and engine thrust. Figure 29 shows the relationship between the momentum coefficient C_μ and the internal duct pressure of the CCW. Figure 30 then provides the exhaust turning angle corresponding to different thrust levels and CCW duct pressure as determined under tunnel static conditions. For the conditions being considered (C_μ = 0.322 giving P_{T_D} = 60 in. Hg, (20.0 X 10^4 N/m^2) and C_T = 1.44 giving T = 59.6 lb (265.0 N)), the engine exhaust is deflected 89 deg. With the model at an angle of attack of 24 deg when a $C_{L_{max}}$ of 5.1 is

generated, the lift due to circulation is 3.8. This is shown in Figure 31 along with the highest values obtained in the test program for the CCW and USB models. Considering that the CCW/USB was operating at a lower C_μ value than that of the CCW alone, and without the demonstrated benefits of the tip sails, the CCW/USB shows the best potential for generating the circulation lift closest to the theoretical maximum.

A feature of the CCW/USB, as is the case with CCW, is that an aircraft using this combination is not required to contend with the high drag of the extended trailing edge flaps and deflected thrust during the takeoff roll, as is so with USB. The procedure would entail using all thrust for acceleration until lift-off, when the CCW would be used to vector the engine thrust to some predetermined position, thereby enhancing the circulation lift and adding the thrust component for immediate lift-off. The CCW/USB combination also has potential for vertical flight because, as shown in Figure 30, the engine exhaust can be vectored up to 165 deg.

CONCLUSIONS

Low aspect ratio wings using powered-lift augmentation have the potential to provide good STOL performance. The CCW/USB configuration has the greatest potential in terms of lift augmentation and versatility for possible modes of operation.

The lift augmentation from the increased circulation due to the CCW trailing edge and that of the deflected USB exhaust flow produced a C_L of 5.1. The CCW/USB model showed an increase of 43-percent in circulation lift (thrust components removed) at $C_\mu = 0.332$. This value of C_μ was the maximum available when simultaneously operating the trailing edge blowing and the propulsion simulator because of a limitation in supply air.

The USB configuration developed a C_L of 4.7. With the thrust component removed, this configuration demonstrated an increase of 28 percent in lift due to circulation.

The CCW configuration developed a C_L of 4.0 with the lift due to circulation being increased by 51-percent at $C_\mu = 0.42$.

The difference in percentage increase in lift due to circulation, between the CCW/USB and CCW alone, is clouded by the fact that the limited supply air restricted the CCW/USB model to a lower C_μ value. This was due to the need to operate both the propulsion simulator and the trailing edge blowing simultaneously off the same source of supply air. The gains of the CCW and USB separately suggest that, with an appropriate air supply, the CCW/USB would be even more effective than demonstrated. Further, the CCW/USB combination has the versatility of thrust vector control by a nonmechanical device to enhance its operational options.

The use of wing tip sails reduced the induced drag factor by 30 to 35 percent while allowing for a moderate increase in C_L. Although the tip sails may not be the best configuration for utilizing the tip vortex, results indicate that wing tip devices are effective on low aspect ratio wings.

Figure 1 - Semispan Wing-Fuselage Model Configurations

NOMINAL ASPECT RATIO	CHORD		SWEEP (deg)		
	TIP	ROOT	L.E.	T.E.	SEMISPAN
3	8.40 in. (21.34cm)	18.34 in. (46.58cm)	25.8	0	1.91 ft (0.582m)
4	6.42 in. (16.31cm)	18.34 in. (46.58cm)	25.8	0	2.12 ft (0.646m)

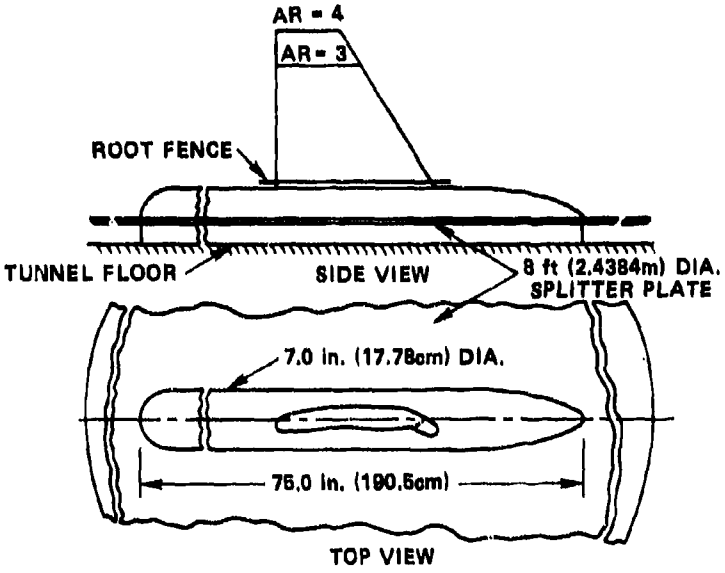

Figure 1a - Semispan Wing-Fuselage Model and Groundboard

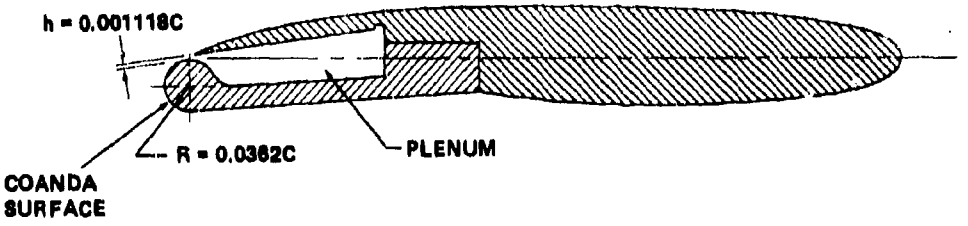

Figure 1b - Circulation Control Wing Configuration

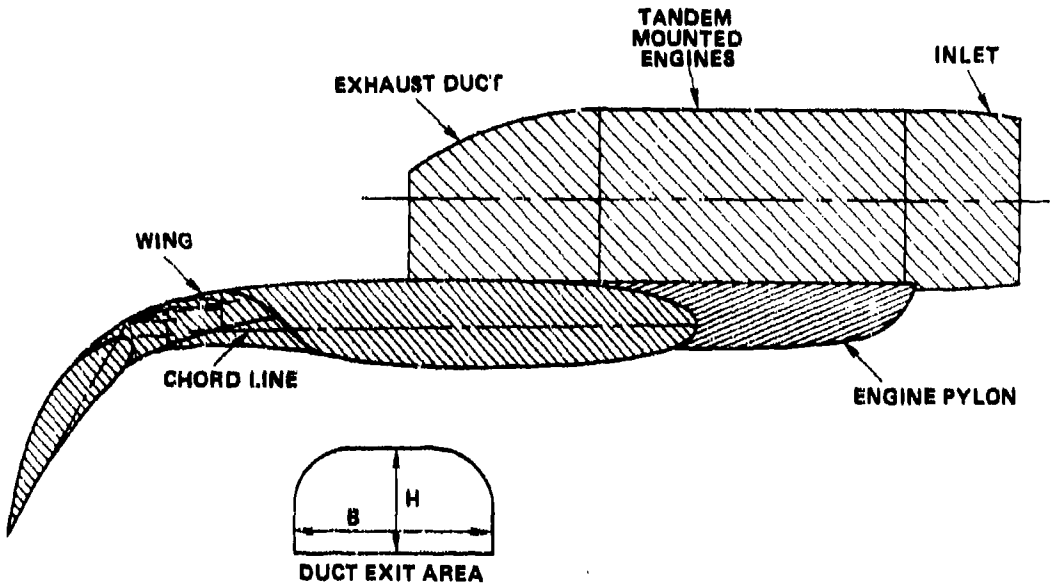

Figure 1c - Upper Surface Blowing Configuration

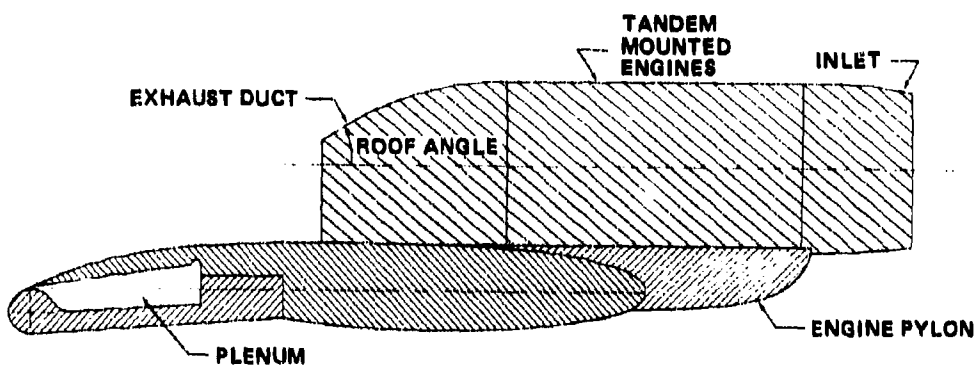

Figure 1d - Circulation Control Wing/Upper Surface
Blowing Configuration

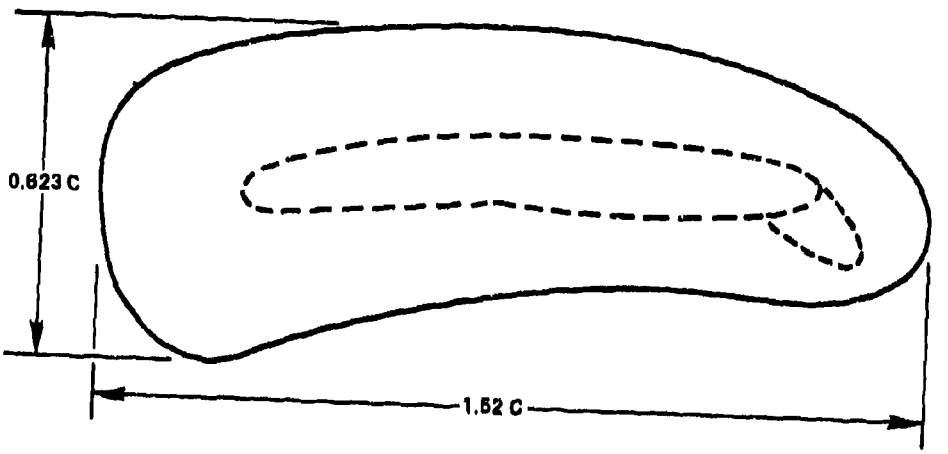

WING TIP PLATE

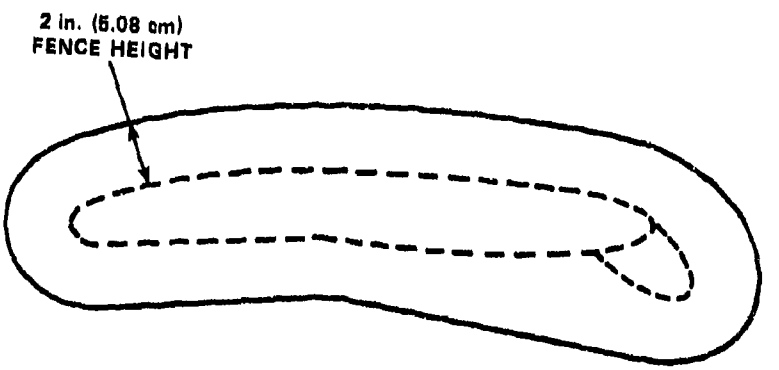

WING ROOT PLATE

Figure 1e - Wing Tip and Wing Root Fence Configurations

Figure 2 - Semispan Model in USB Configuration

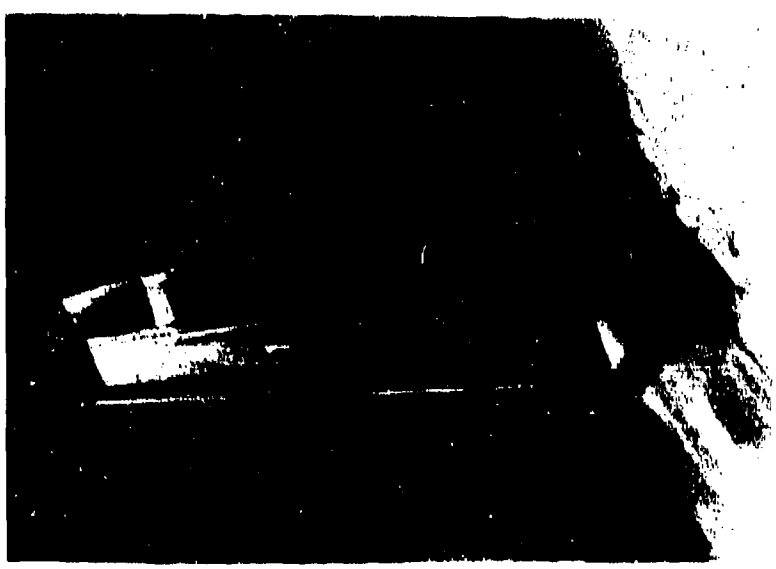

Figure 3 - Semispan Model in CCW Configuration with Wing Tip Fence

Figure 4 - Semispan Model in CCW/USB Configuration

Figure 5 - Supercritical Wing in Smoke Tunnel

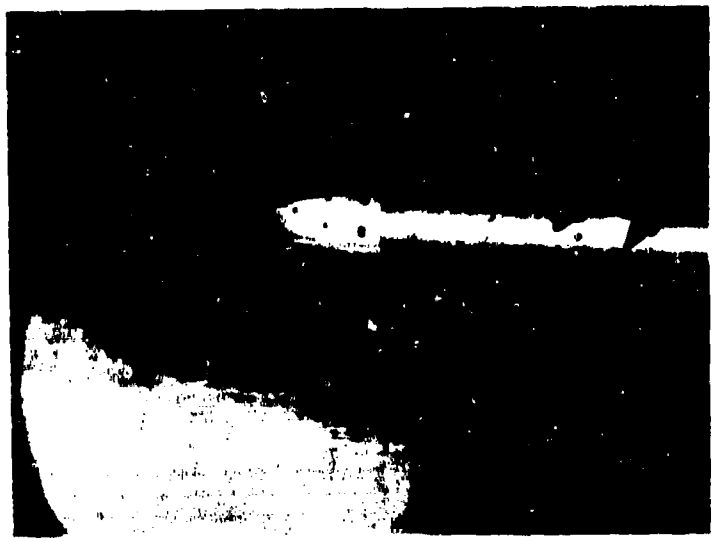

Figure 5a - Wing Tip Sails

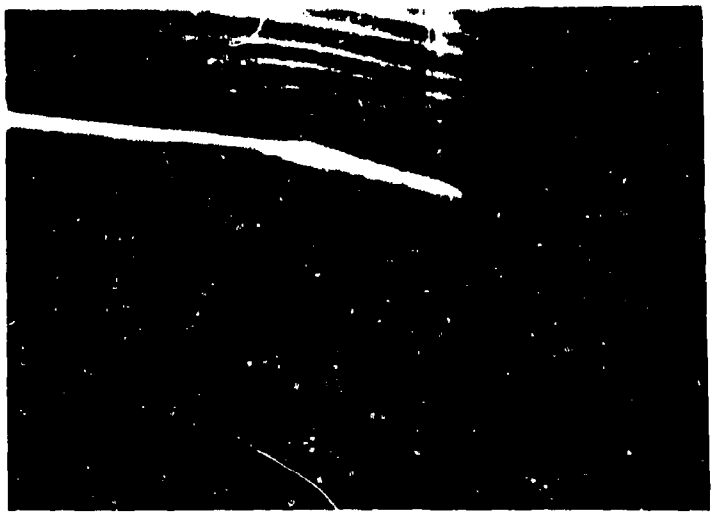

Figure 5b - Wing Tip Vortex (Plain Tip)

Figure 5 (Continued)

Figure 5c - Tip Flow at Stall

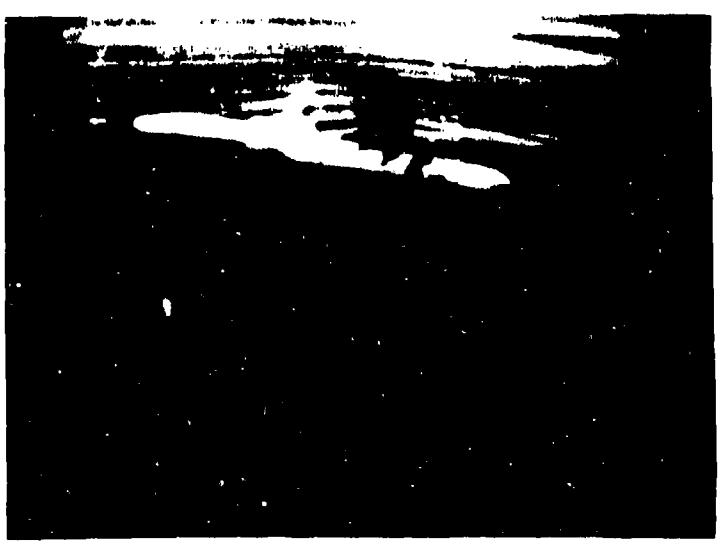

Figure 5d - Tip Vortex as Affected by Sails

Figure 6 - Longitudinal Characteristics of CCW Configuration with Plain Wing Tip, AR = 4, δ_n = 40 Degrees

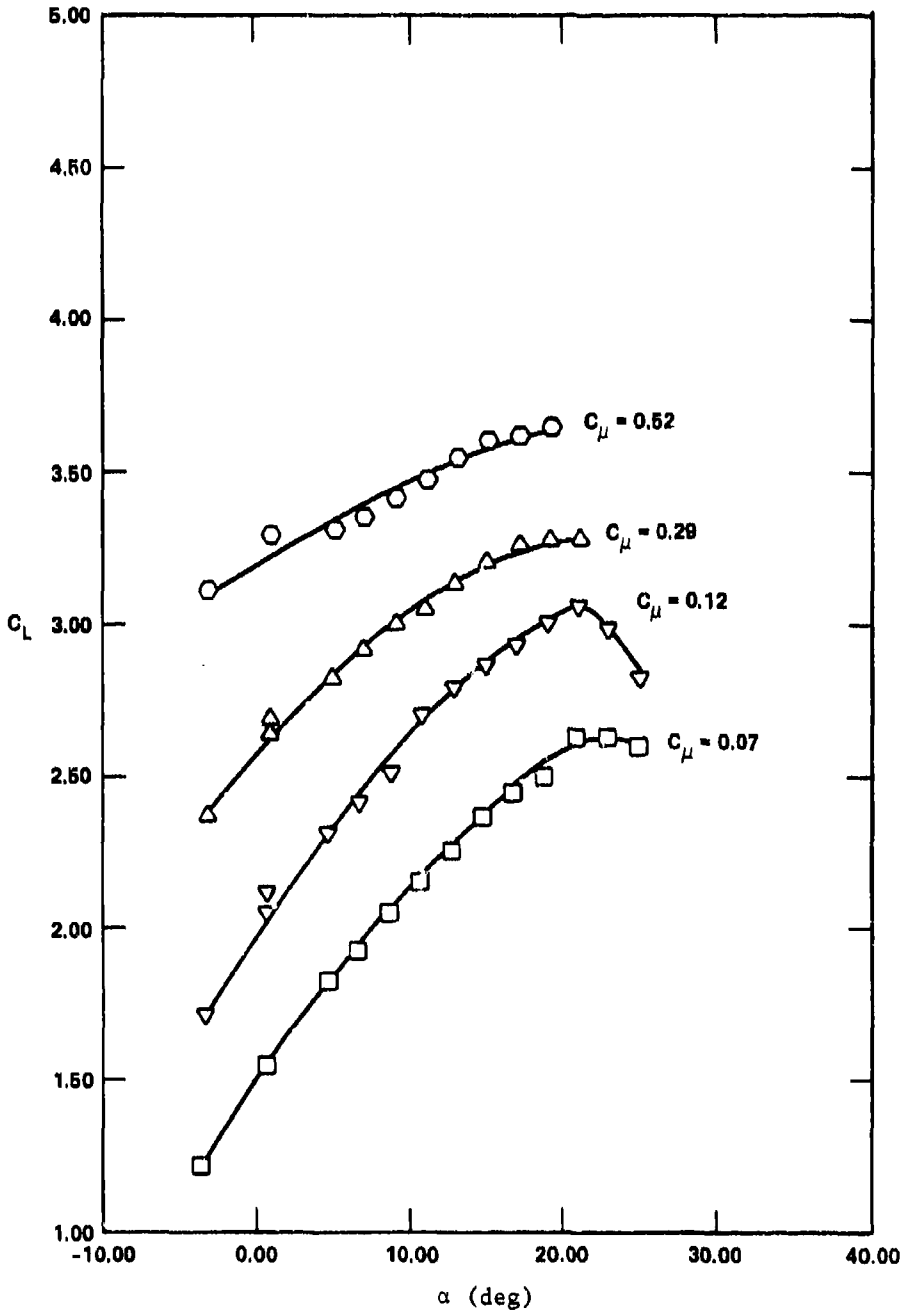

Figure 6a - Lift Curve

Figure 6 (Continued)

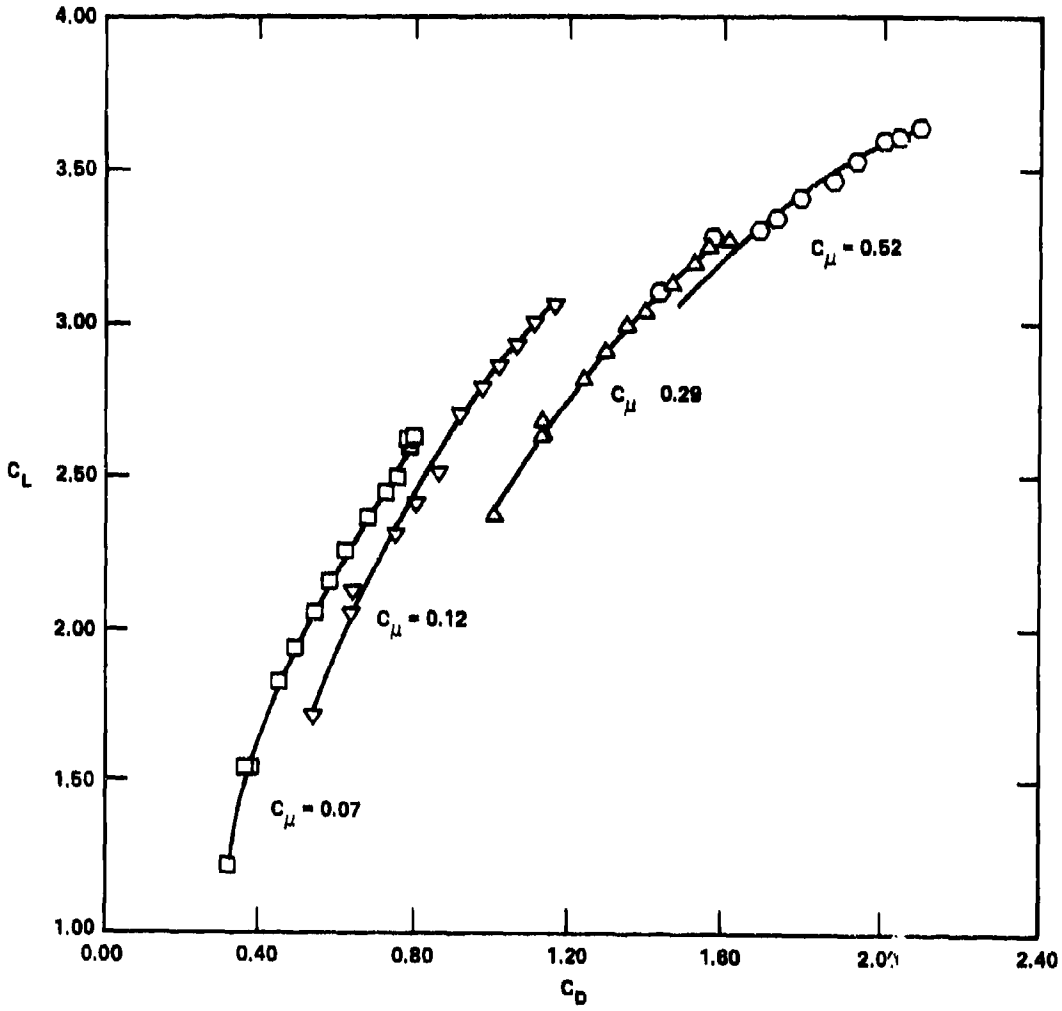

Figure 6b - Drag Polar

Figure 7 - Longitudinal Characteristics of CCW Configuration with Wing Tip Fence, AR = 4, δ_n = 40 Degrees

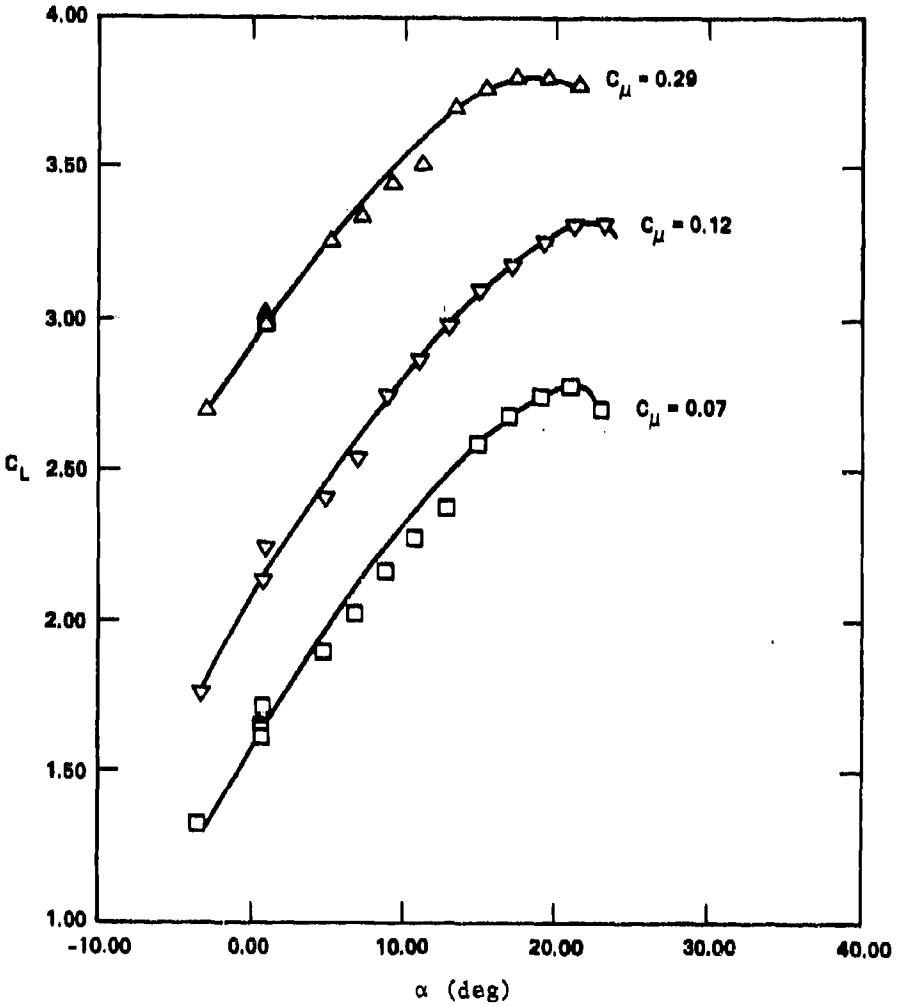

Figure 7a - Lift Curve

Figure 7 (Continued)

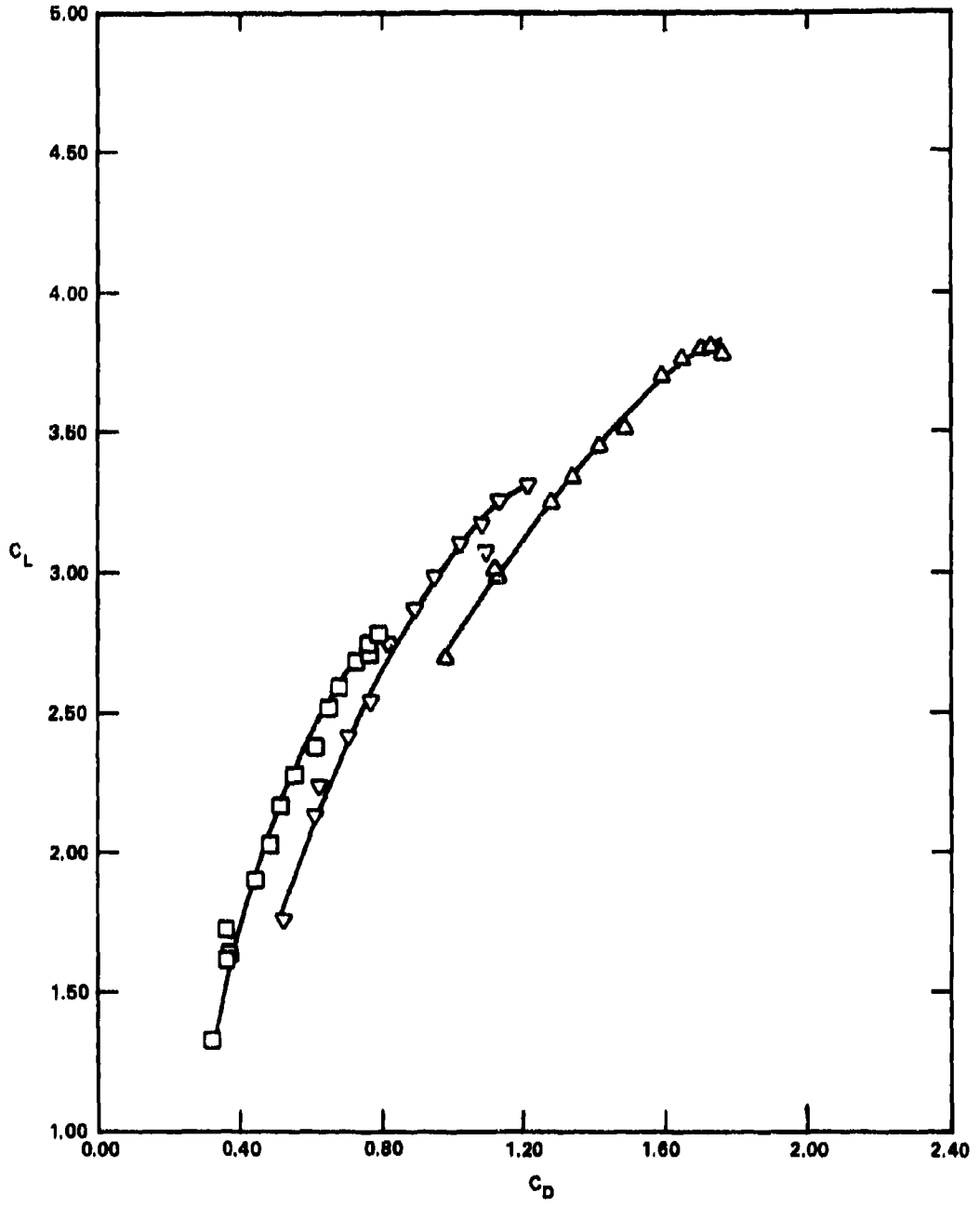

Figure 7b - Drag Polar

Figure 8 - Longitudinal Characteristics of CCW Configuration with Four Tip Sails, AR = 4, δ_n = 40 Degrees

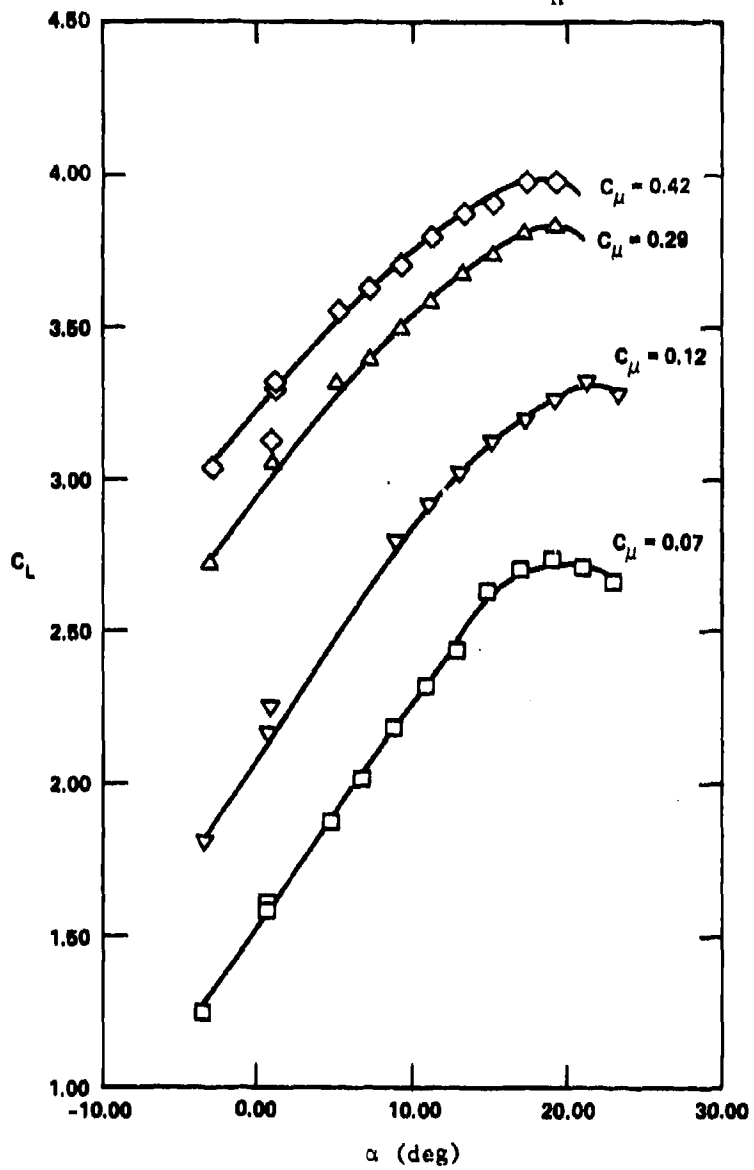

Figure 8a - Lift Curve

Figure 8 (Continued)

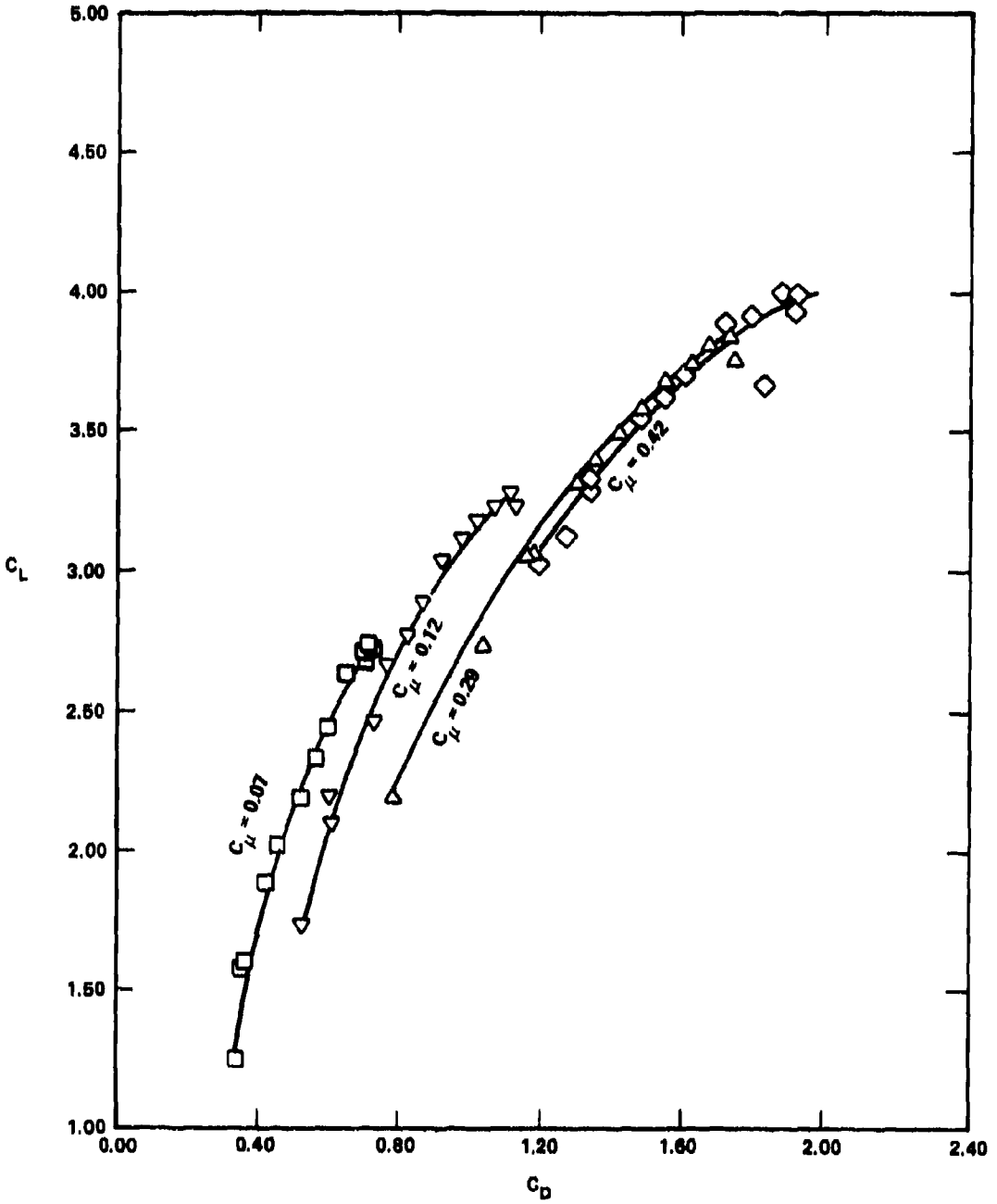

Figure 8b - Drag Polar

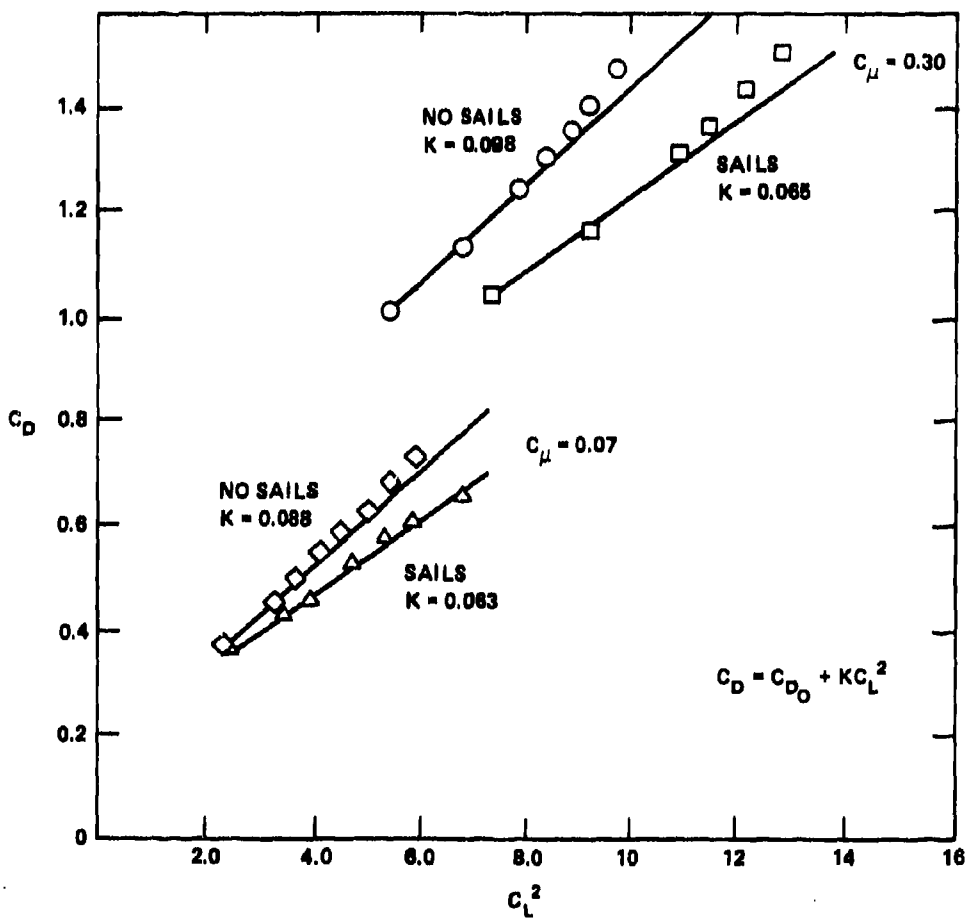

Figure 9 - Effect of Tip Sails on Induced Drag for CCW Configuration, AR = 4, δ_n = 40 Degrees

Figure 10a - Nozzle Insert and Tip Sails, δ_f = 40 Degrees

Figure 10b - Plain Tip, δ_f = 60 Degrees

Figure 10c - Outboard Double Slotted Flaps, Tip Fence, δ_f = 60 Degrees

Figure 10 - Oil Flow for USB Model, AR = 4, Static Tunnel Conditions

Figure 11 - Longitudinal Characteristics of USB Configuration with Wing Tip Fence, AR = 4, δ_f = 40 Degrees, δ_n = 40 Degrees

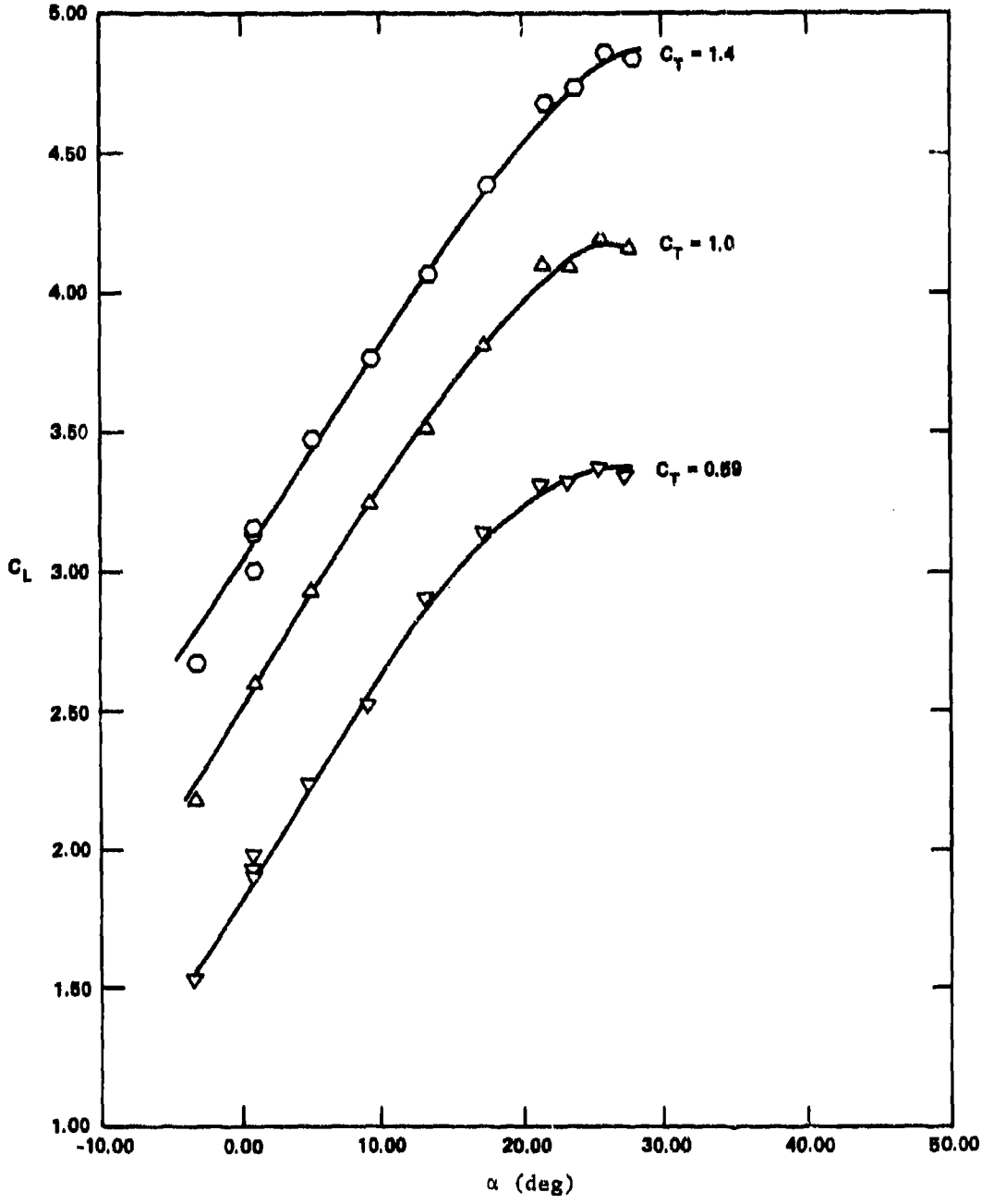

Figure 11a - Lift Curve

Figure 11 (Continued)

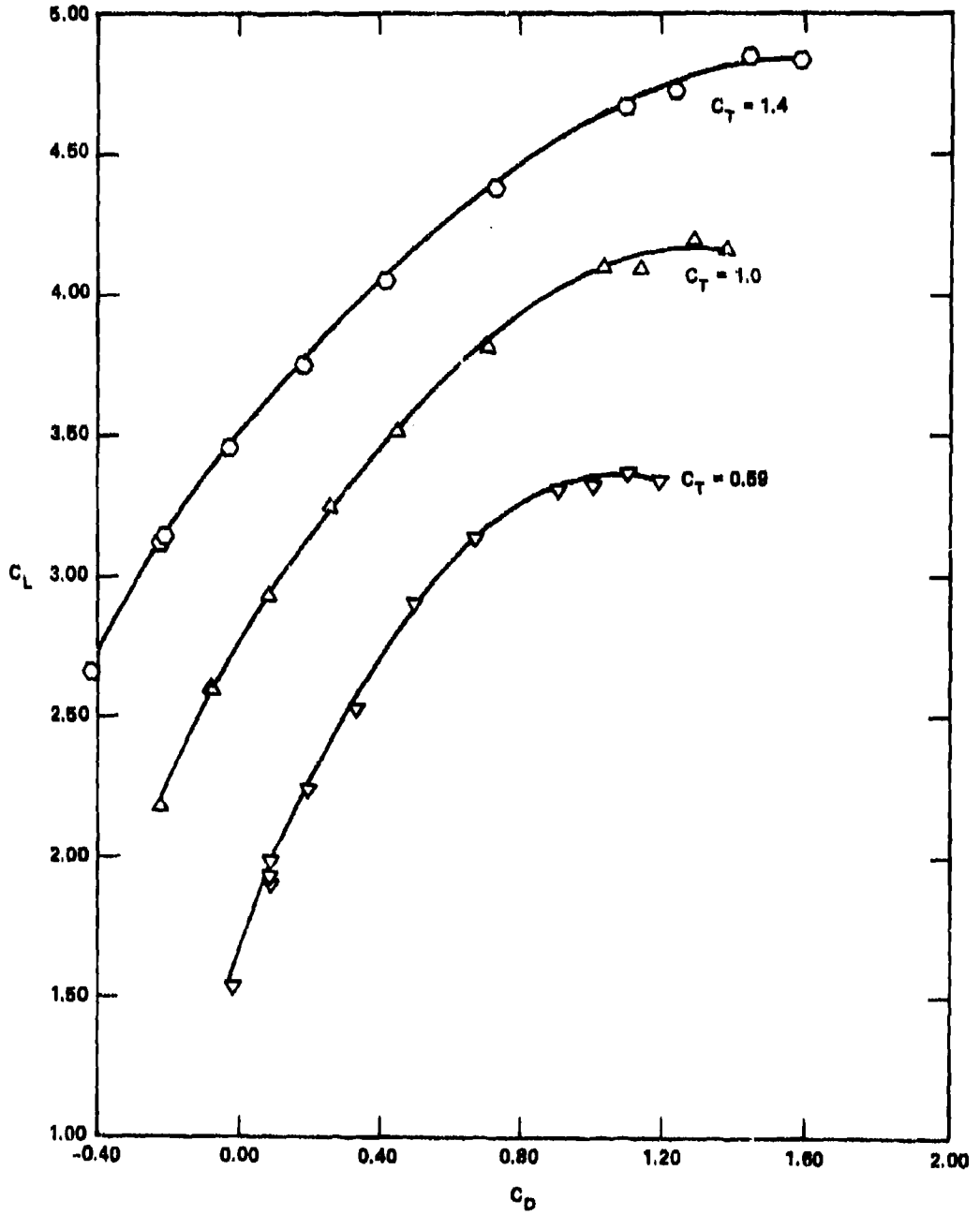

Figure 11b - Drag Polar

Figure 12 - Longitudinal Characteristics of USB Configuration with Four Tip Sails, AR = 4, δ_f = 40 Degrees, δ_n = 40 Degrees

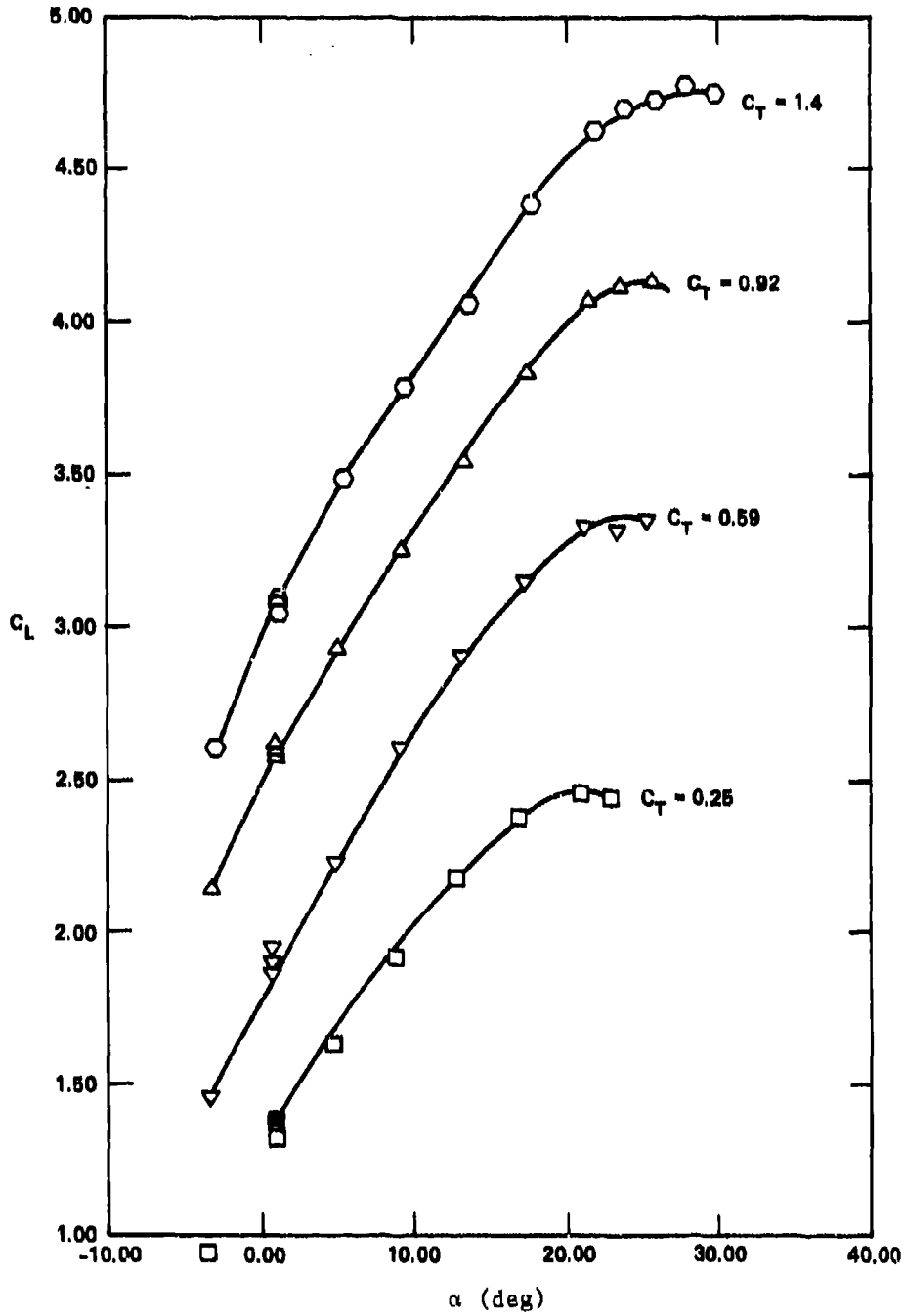

Figure 12a - Lift Curve

Figure 12 (Continued)

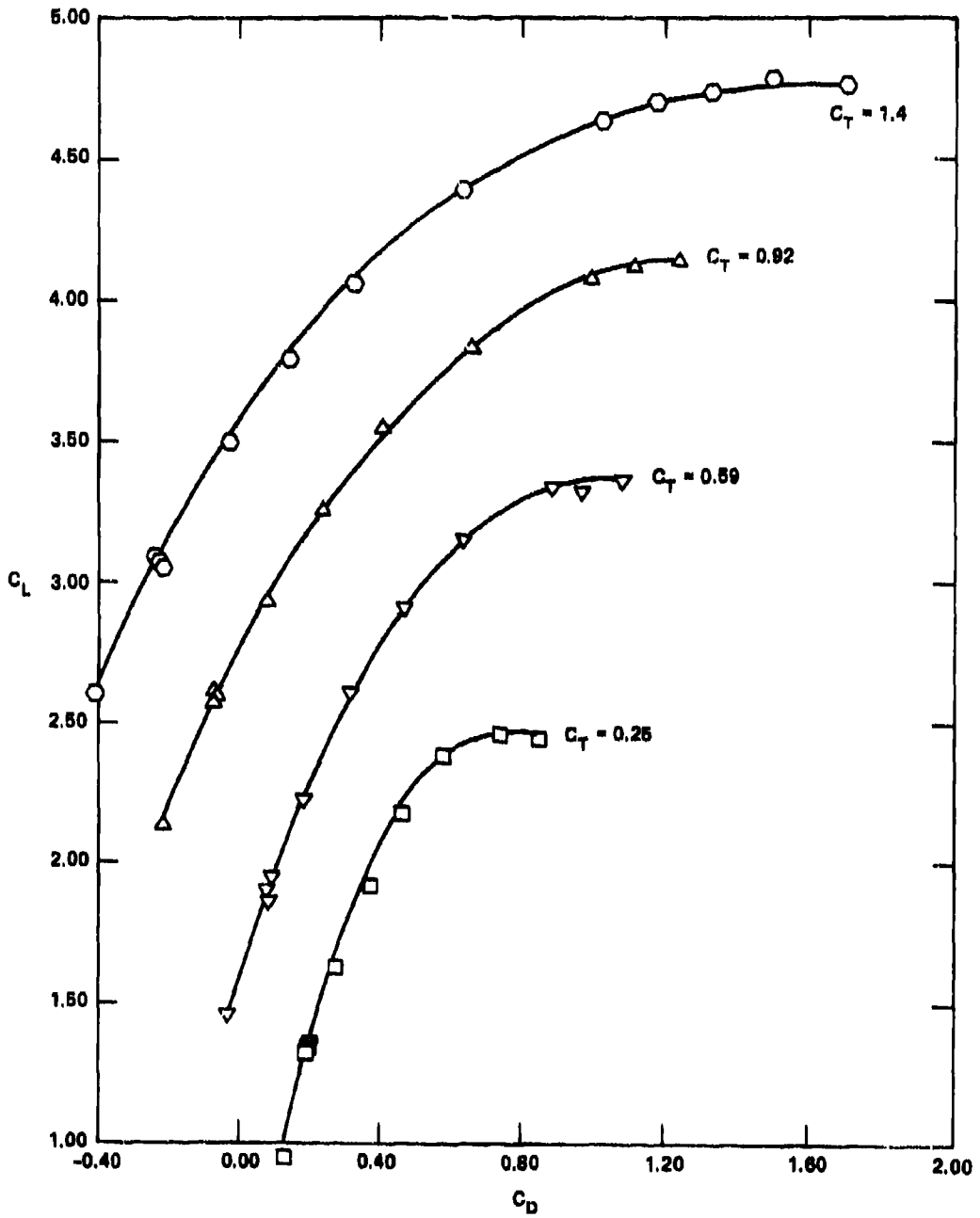

Figure 12b - Drag Polar

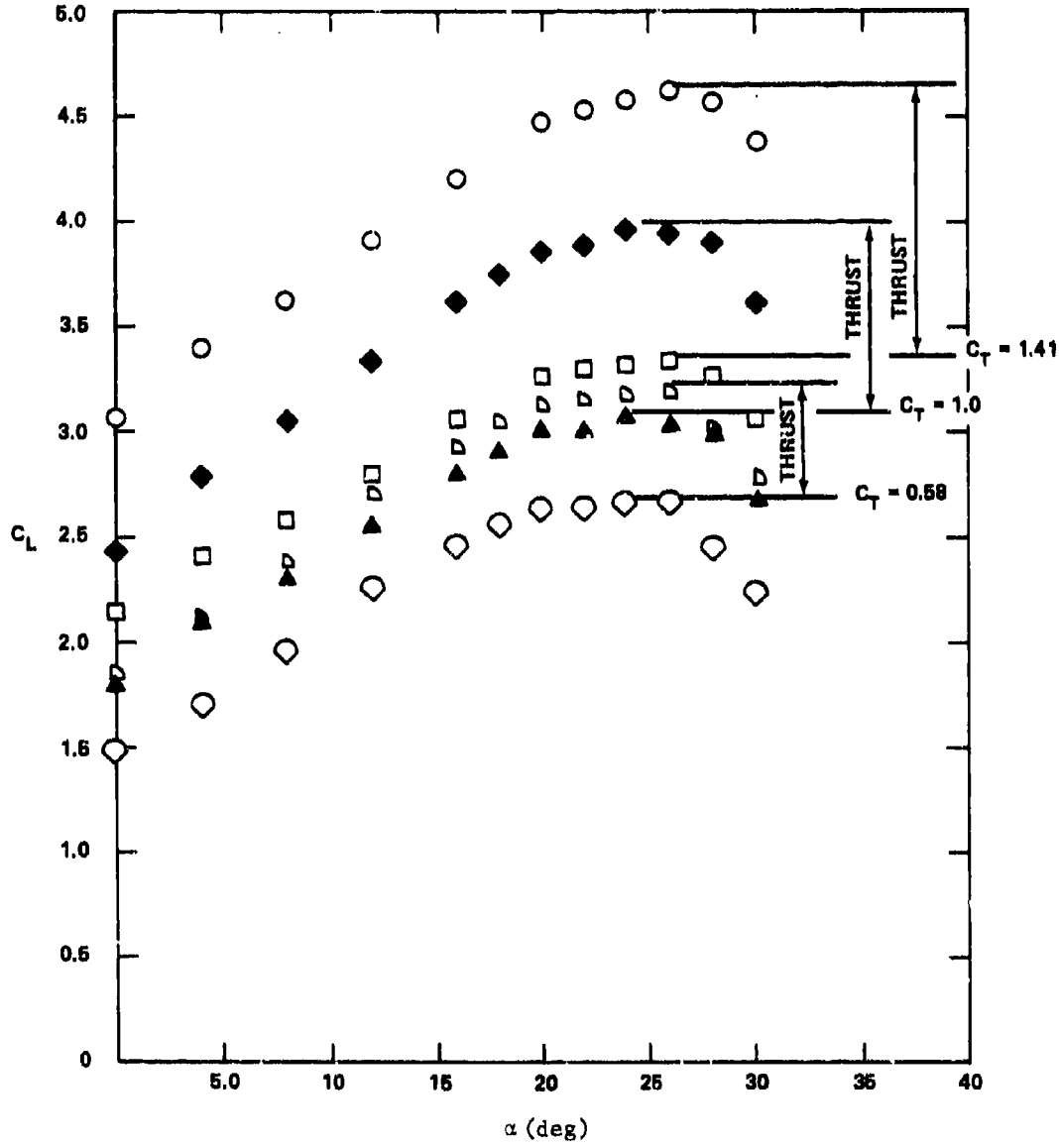

Figure 13 - Lift Components for USB Configuration with Tip Sails, AR = 4, δ_f = 40 Degrees, δ_n = 40 Degrees

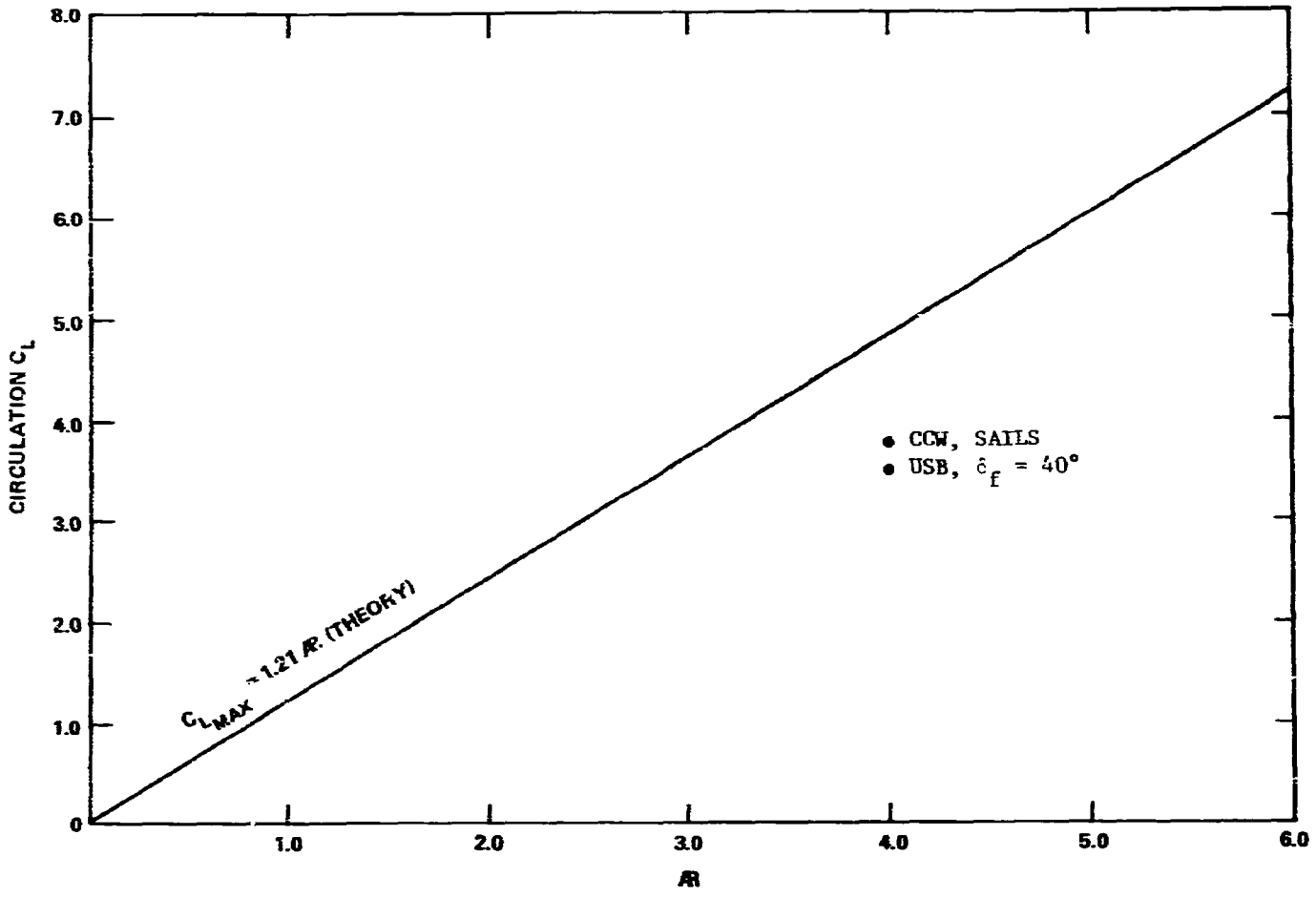

Figure 14 - Circulation Lift of CCW and USB

Figure 15 - Longitudinal Characteristics of USB Configuration with Plain Wing Tip, AR = 4, δ_f = 60 Degrees, δ_n = 40 Degrees

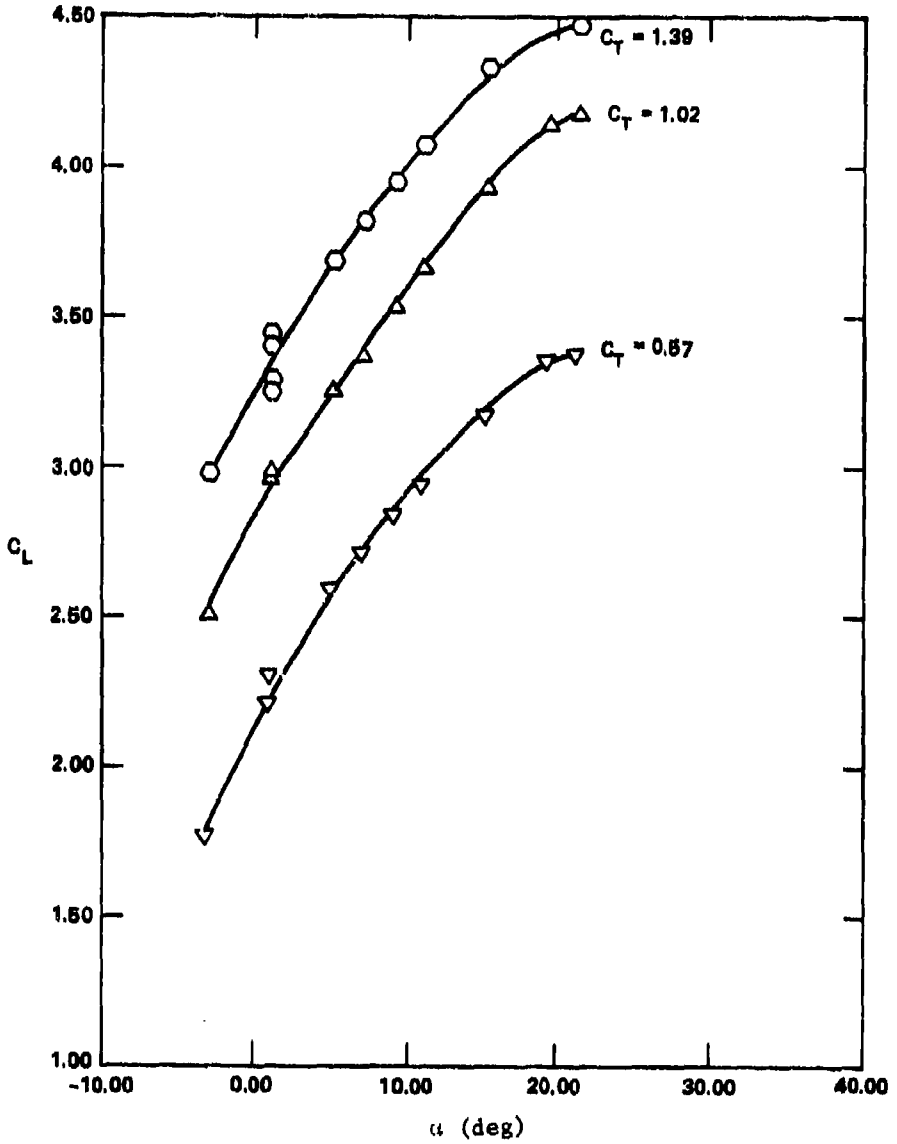

Figure 15a - Lift Curve

Figure 15 (Continued)

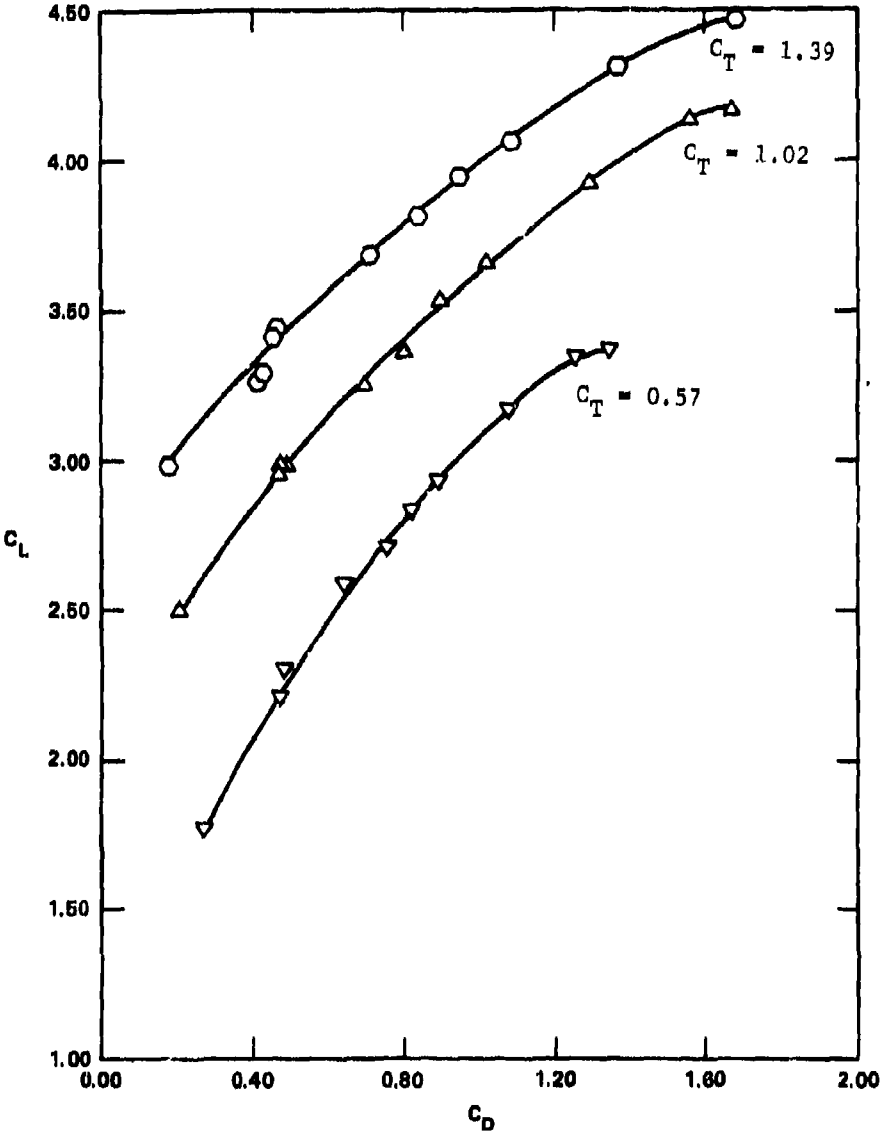

Figure 15b - Drag Polar

Figure 16 - Longitudinal Characteristics of USB Configuration with Four Tip Sails, AR = 4, δ_f = 60 Degrees, δ_n = 40 Degrees

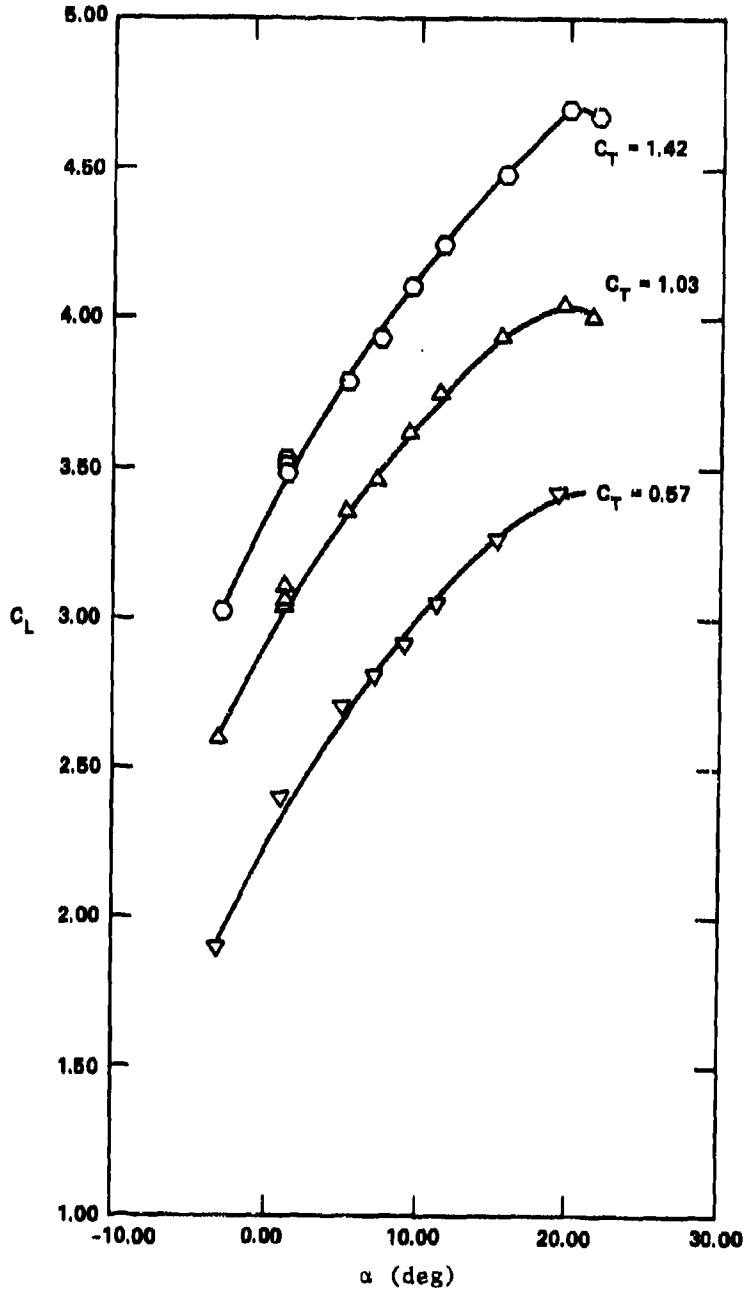

Figure 16a - Lift Curve

Figure 16 (Continued)

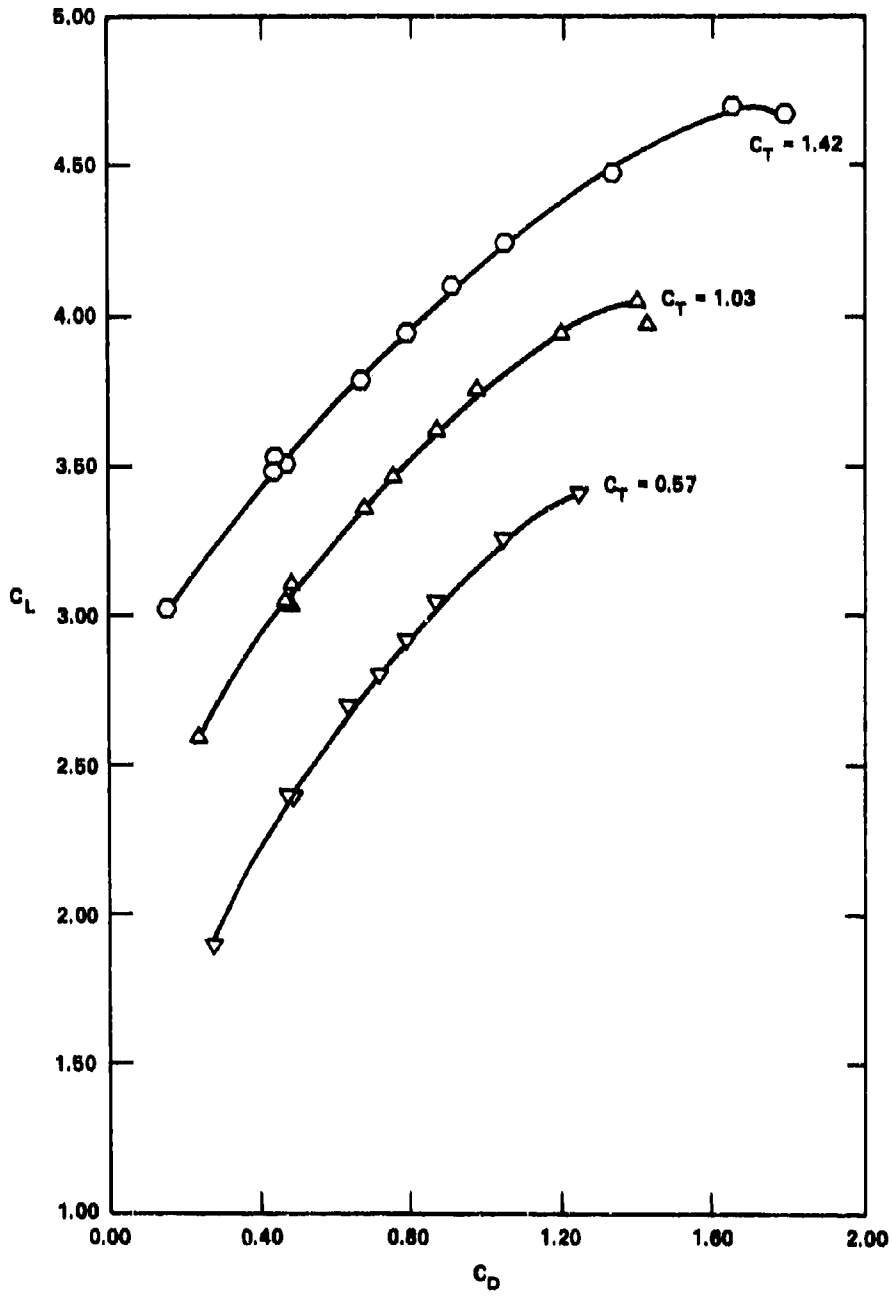

Figure 16b - Drag Polar

Figure 17 - Longitudinal Characteristics of USB Configuration with Wing Tip Fence, AR = 4, δ_f = 60 Degrees, δ_n = 40 Degrees

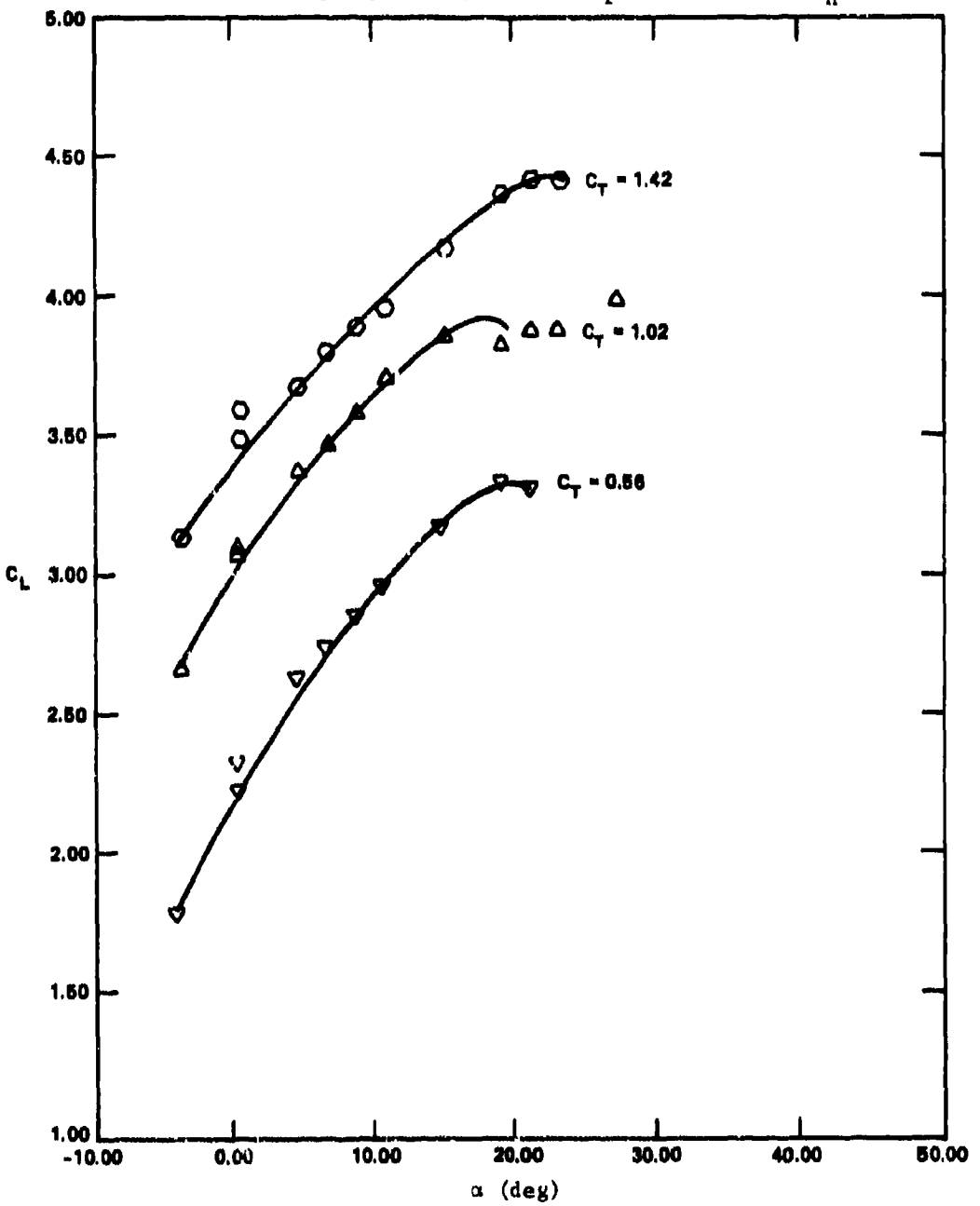

Figure 17a - Lift Curve

Figure 17 (Continued)

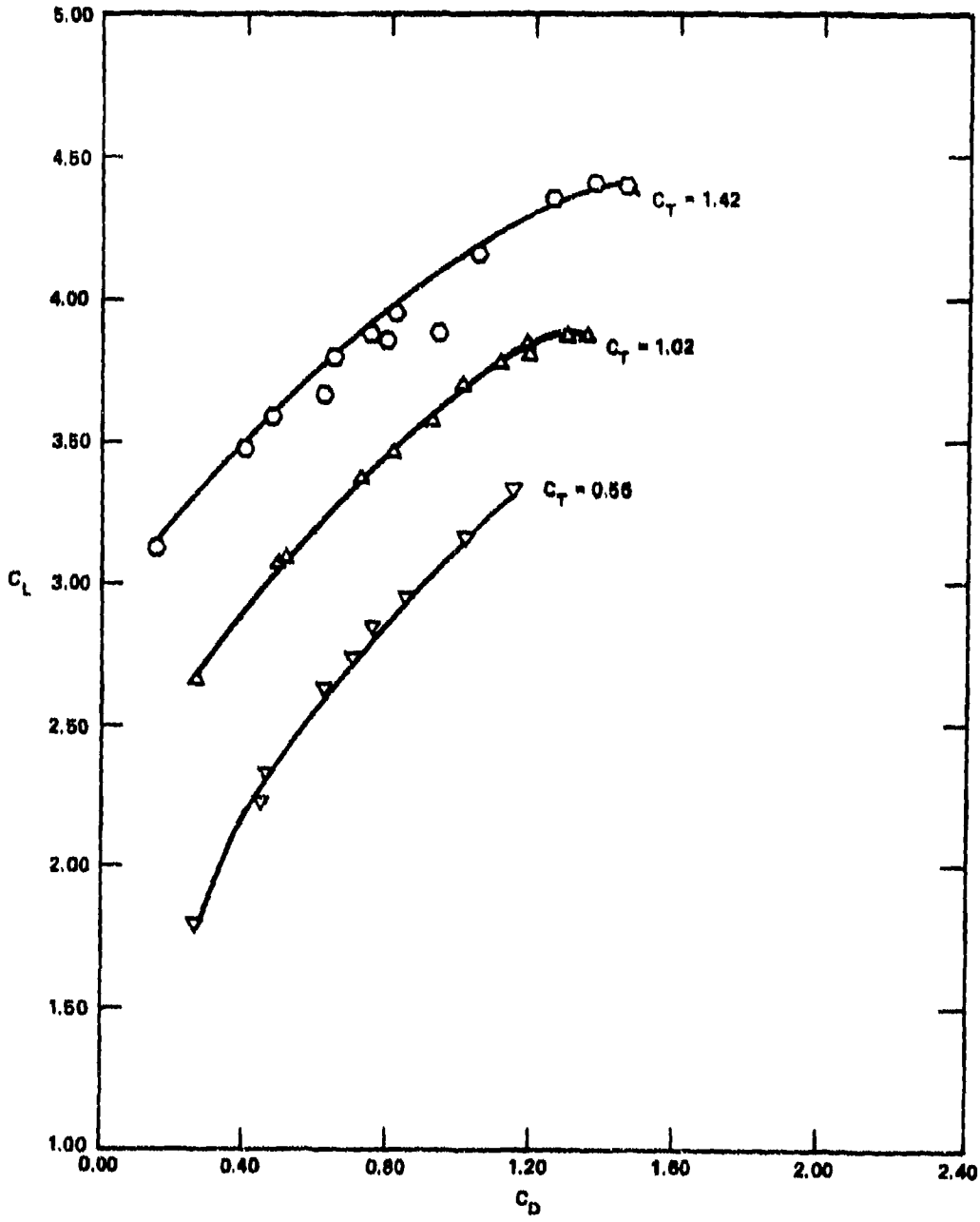

Figure 17b - Drag Polar

Figure 18a - Plain Tip

Figure 18b - Wing Tip Fence

Figure 18c - Wing Tip Sails

Figure 18 - Oil Flow for USB Configuration, AR = 4
δ_f = 60 Degrees, δ_n = 40 Degrees, α = 18 Degrees

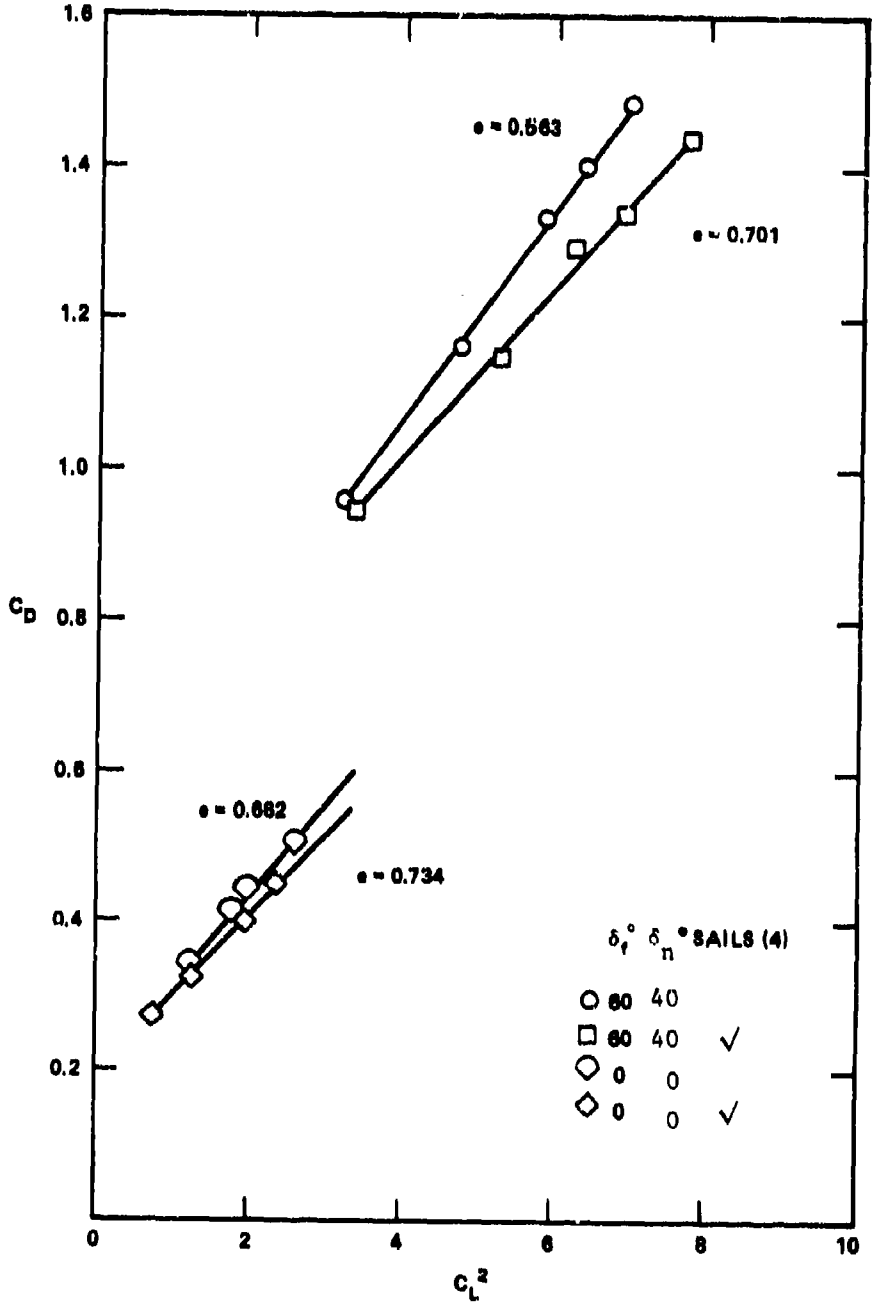

Figure 19 - Effect of Tip Sails on Induced Drag for USB Configuration, AR = 4

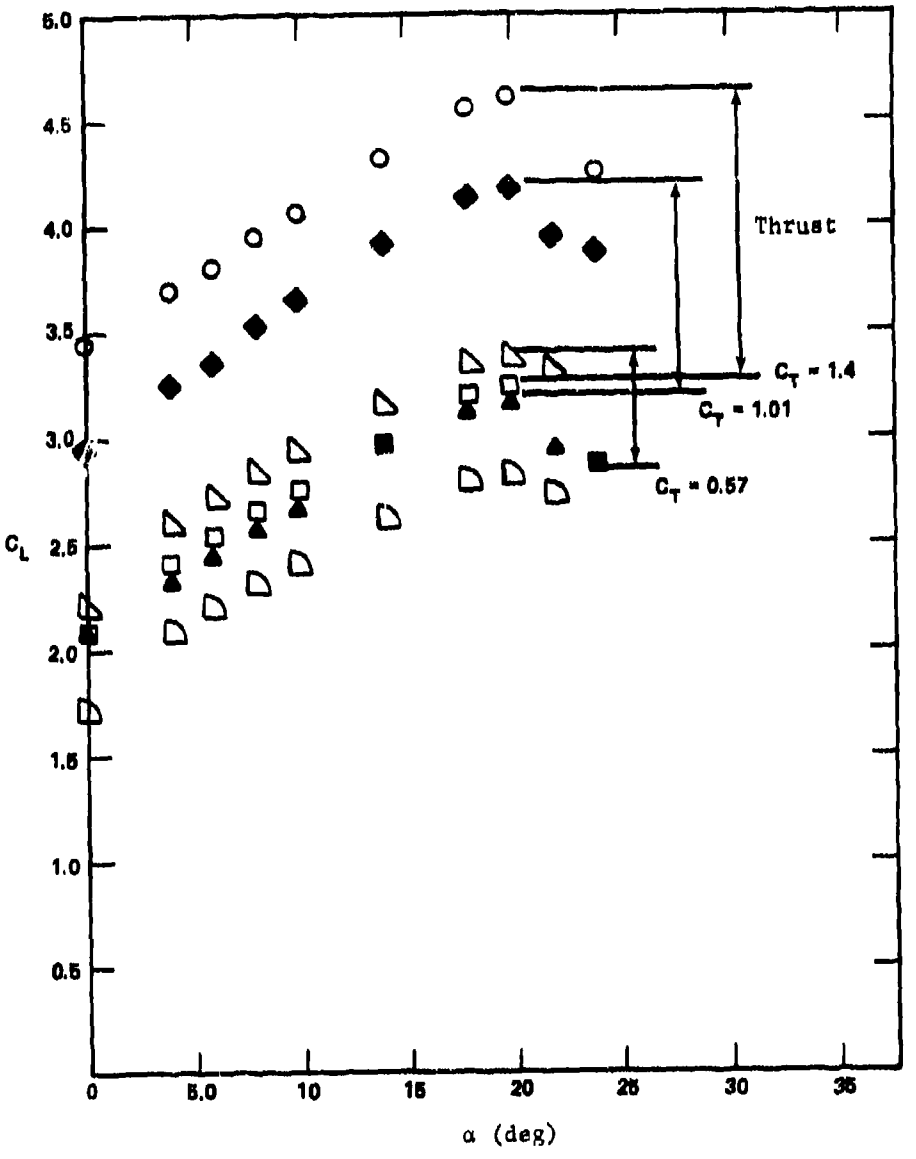

Figure 20 - Lift Components for USB Configuration, AR = 4, δ_f = 60 Degrees, δ_n = 40 Degrees

Figure 21 - Longitudinal Characteristics of USB Configuration with Plain Wing Tip, AR = 4, δ_f = 0 Degrees, δ_n = 0 Degrees

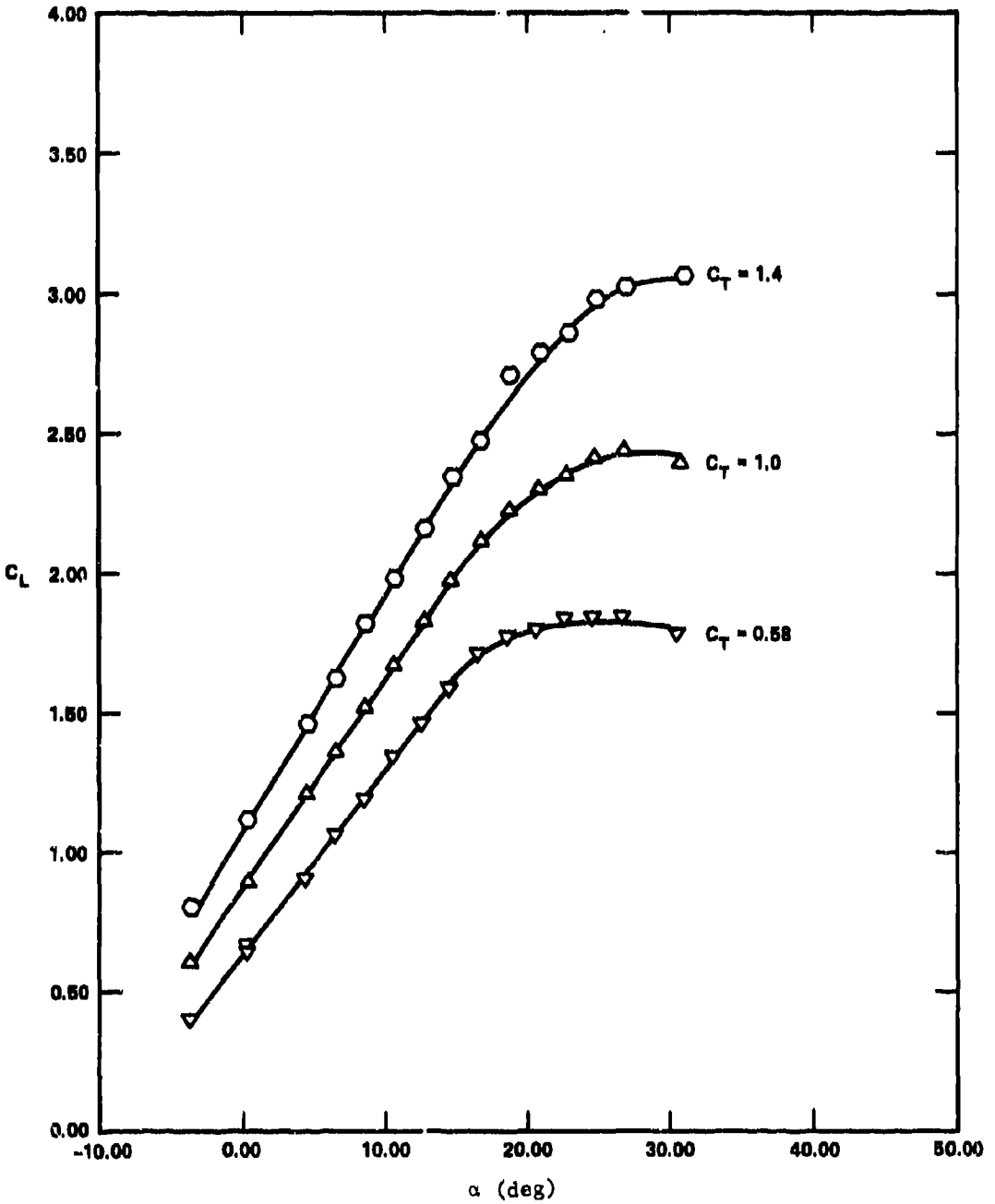

Figure 21a - Lift Curve

Figure 21 (Continued)

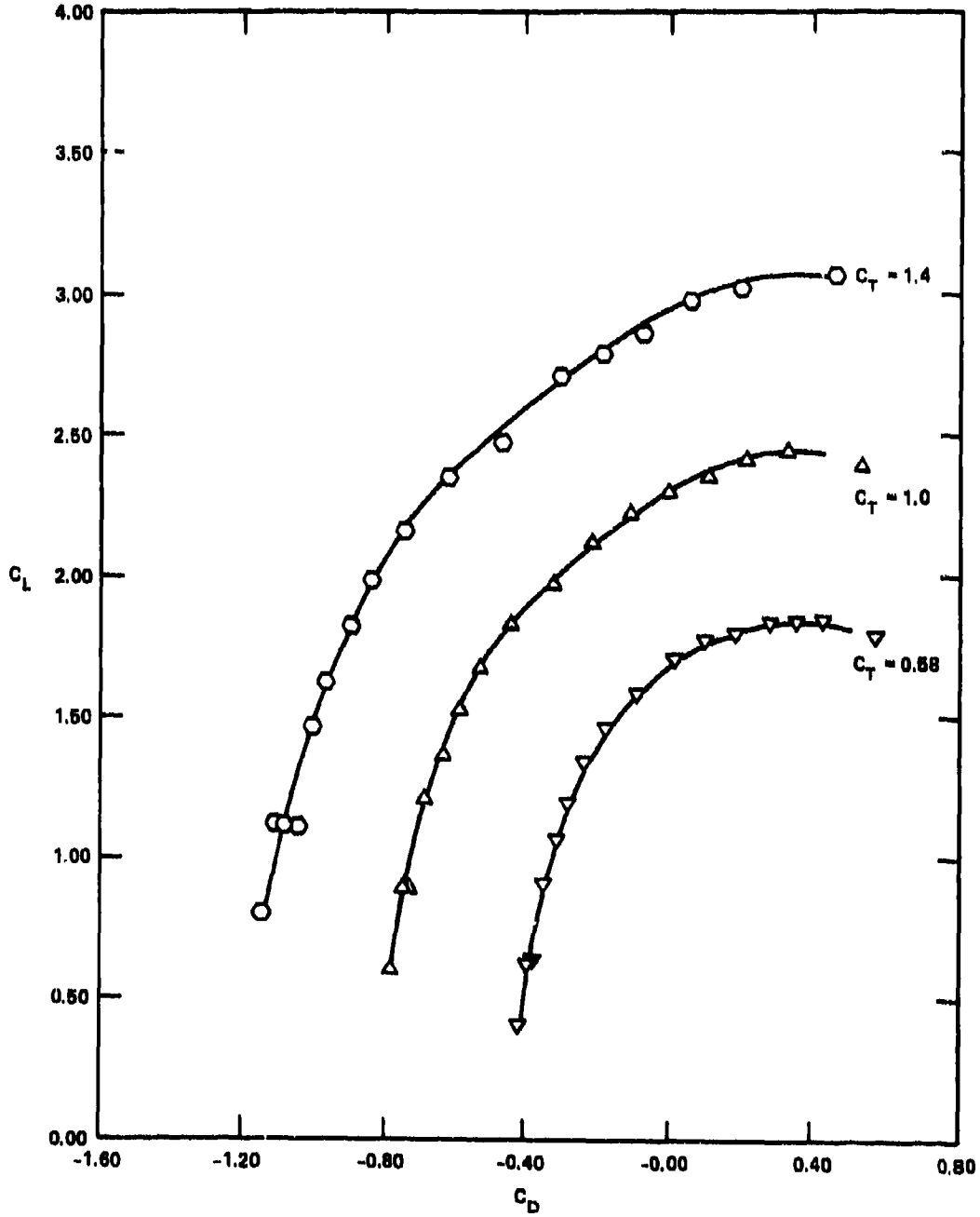

Figure 21b - Drag Polar

Figure 22 - Longitudinal Characteristics of USB Configuration with Wing Tip Fence, AR = 4, δ_f = 0 Degrees, δ_n = 0 Degrees

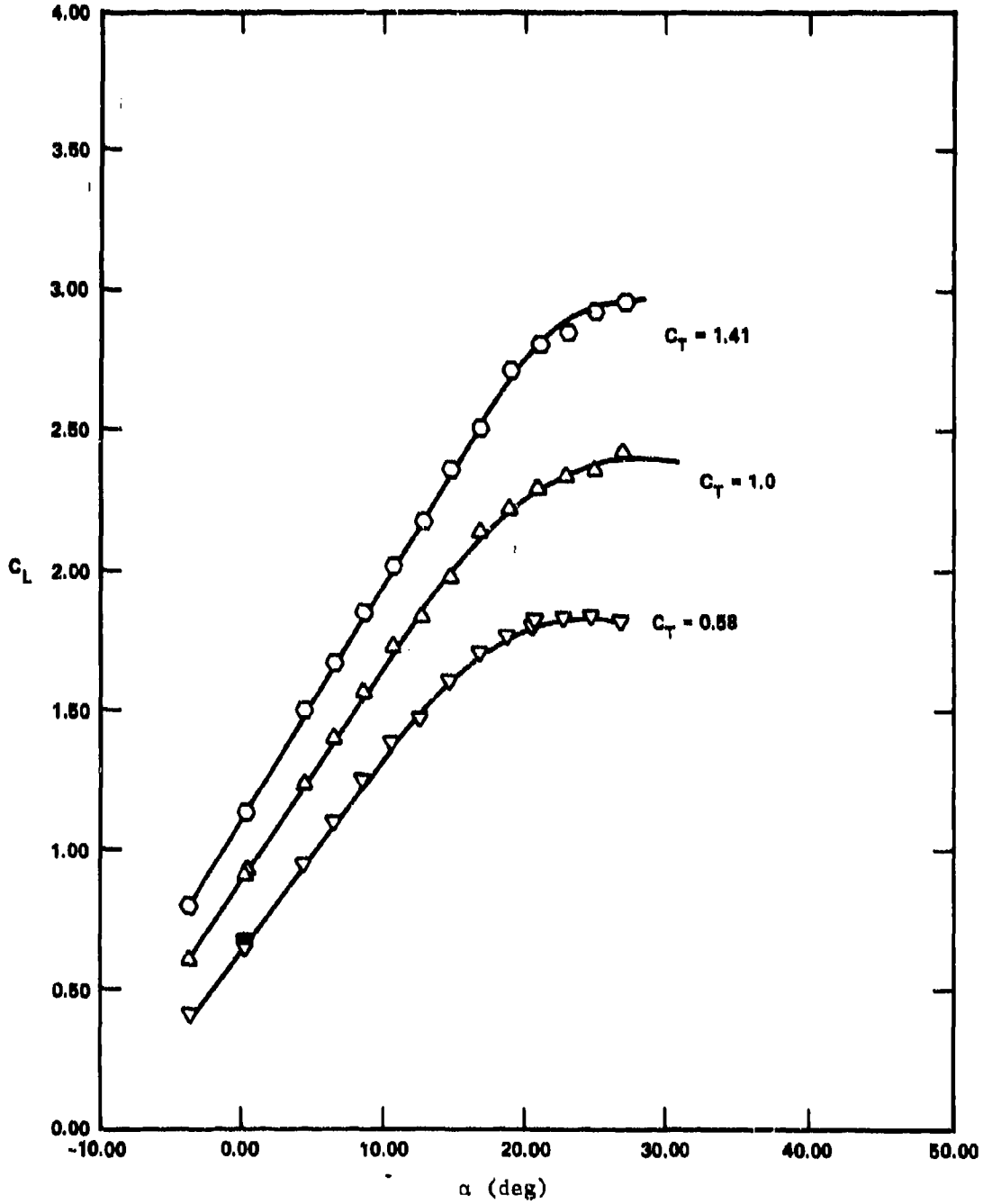

Figure 22a - Lift Curve

Figure 22 (Continued)

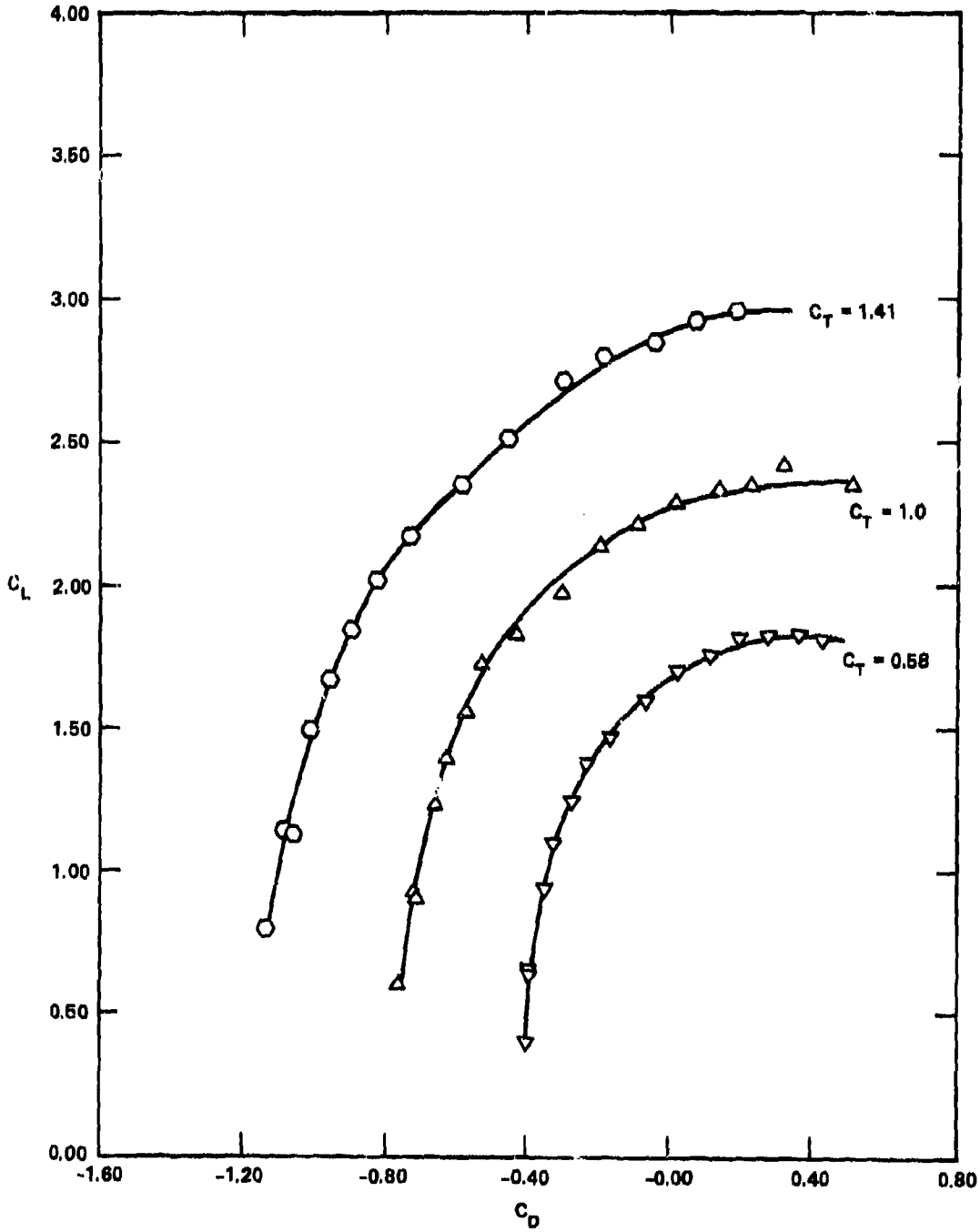

Figure 22b - Drag Polar

Figure 23 - Longitudinal Characteristics of USB Configuration with Wing Tip Sails, AR = 4, δ_f = 0 Degrees, δ_n = 0 Degrees

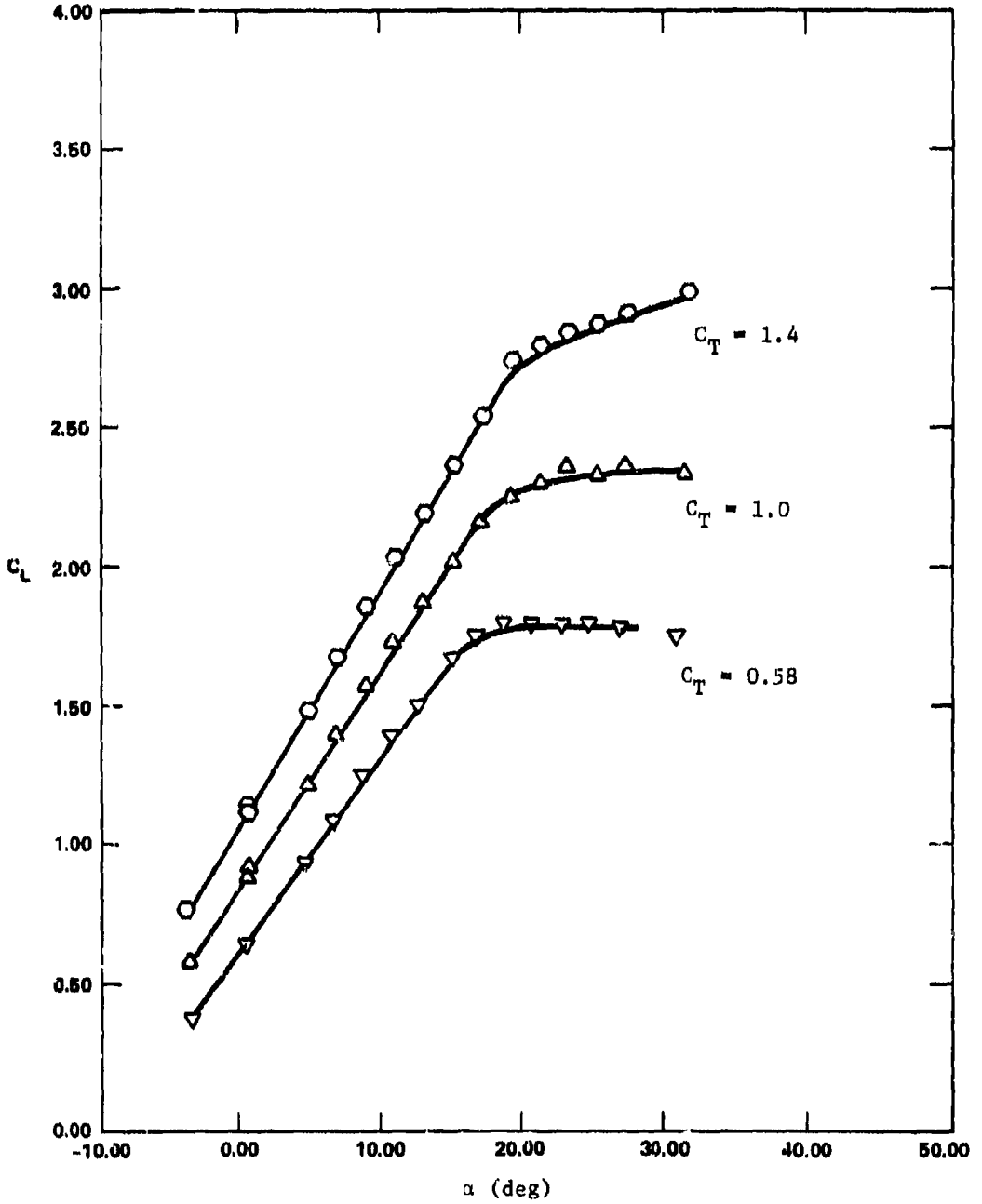

Figure 23a - Lift Curve

Figure 23 (Continued)

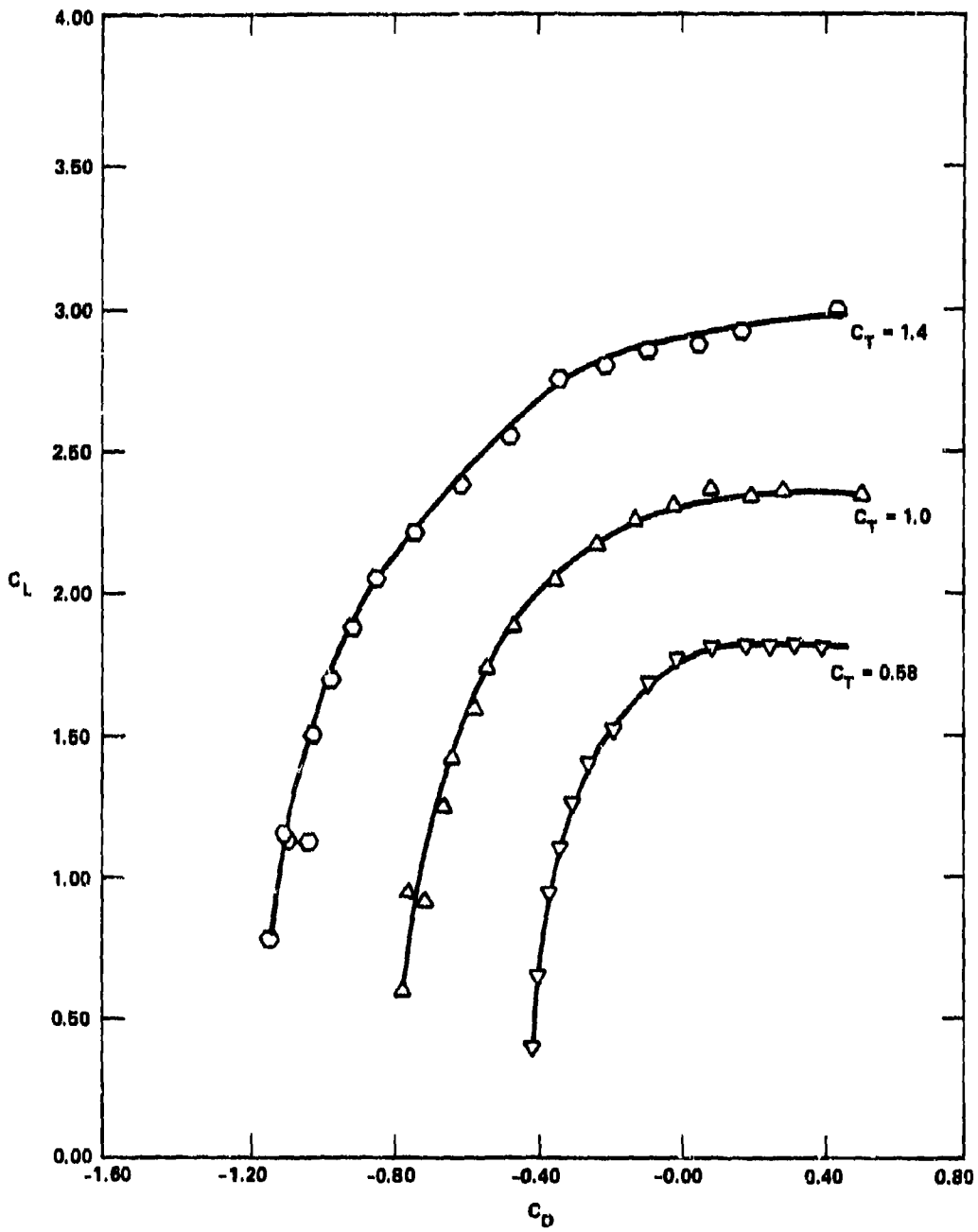

Figure 23b - Drag Polar

Figure 24 - Longitudinal Characteristics of USB Configuration With Plain Wing Tip, AR = 5, δ_f = 0 Degrees, δ_n = 0 Degrees

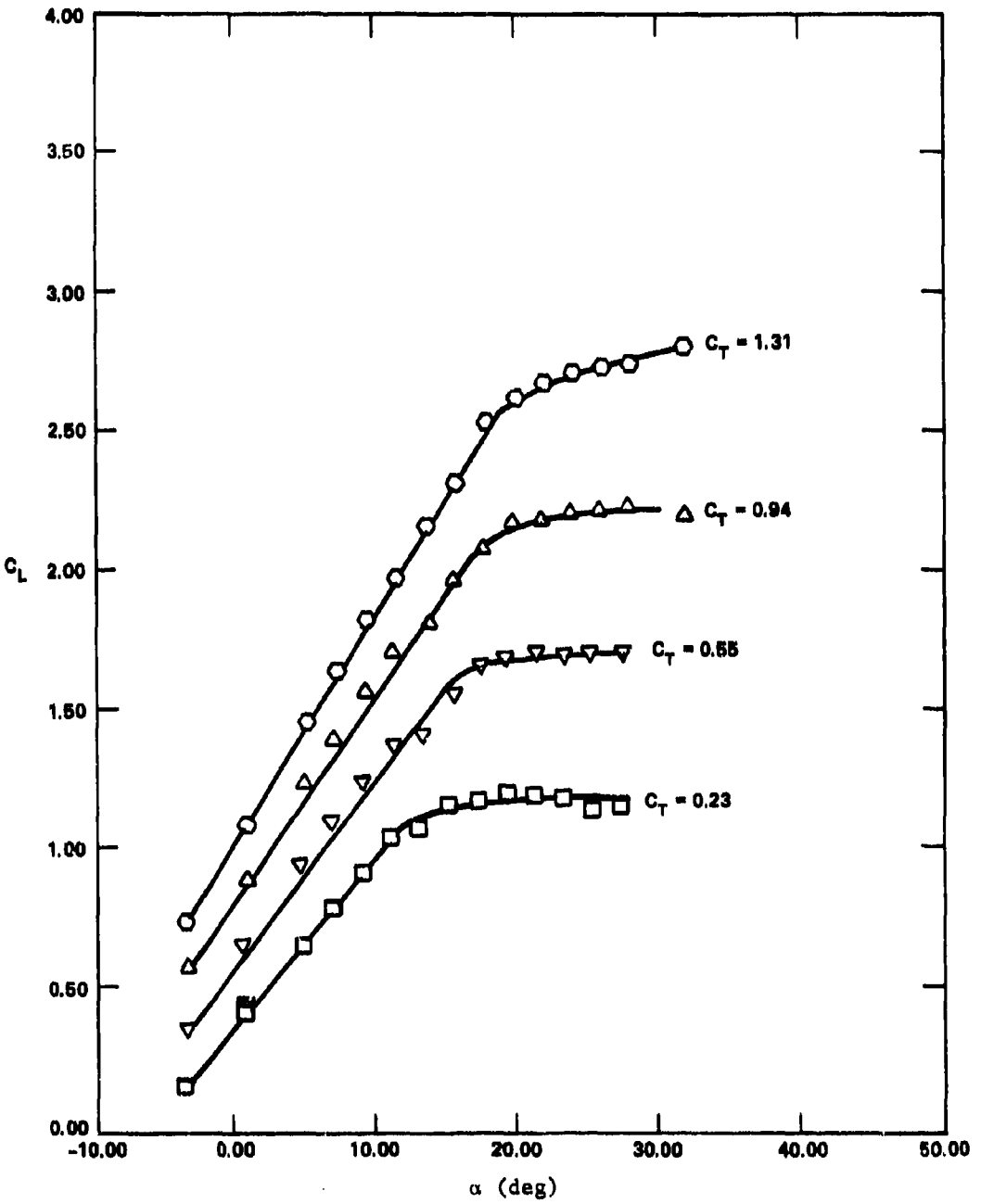

Figure 24a - Lift Curve

Figure 24 (Continued)

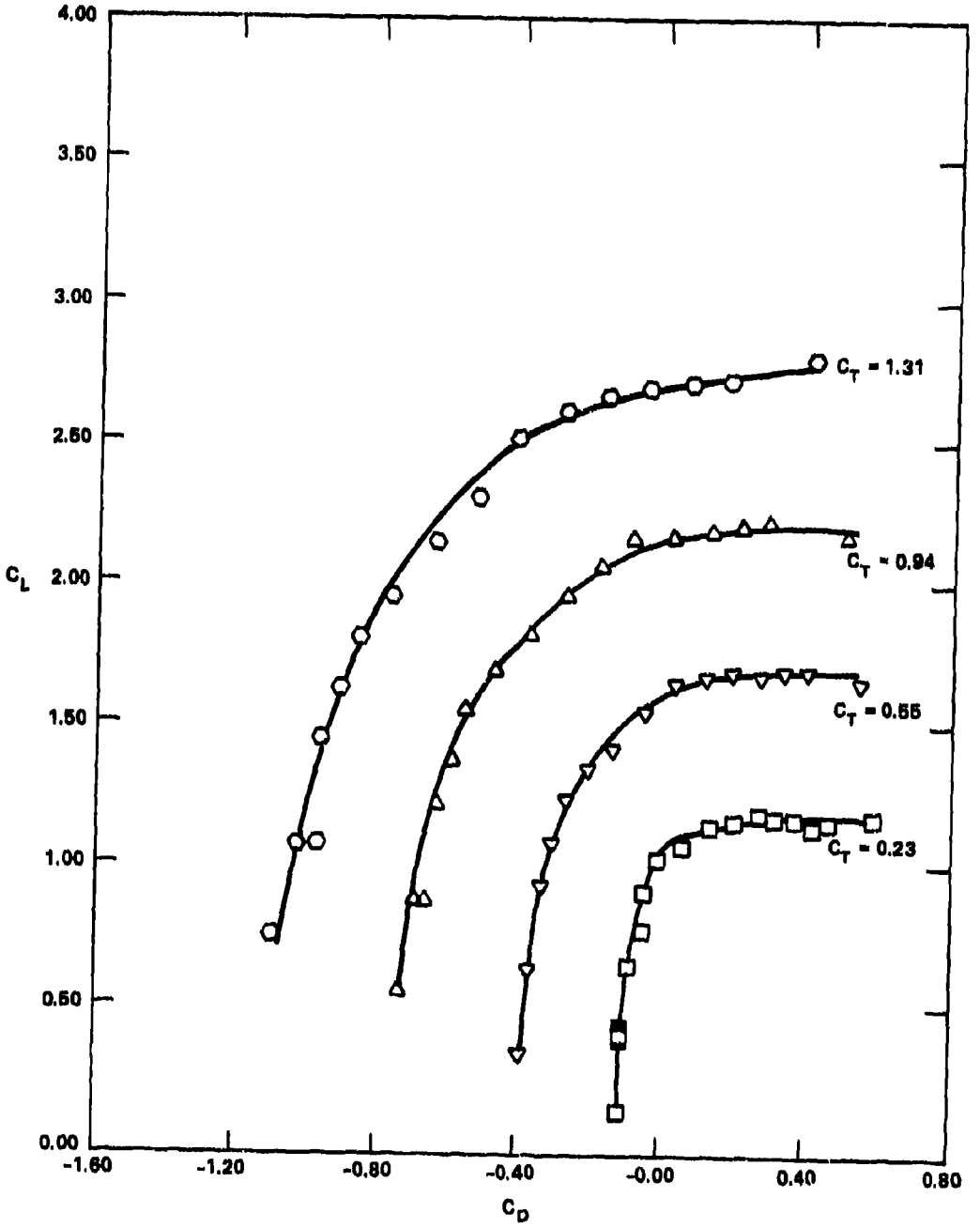

Figure 24b - Drag Polar

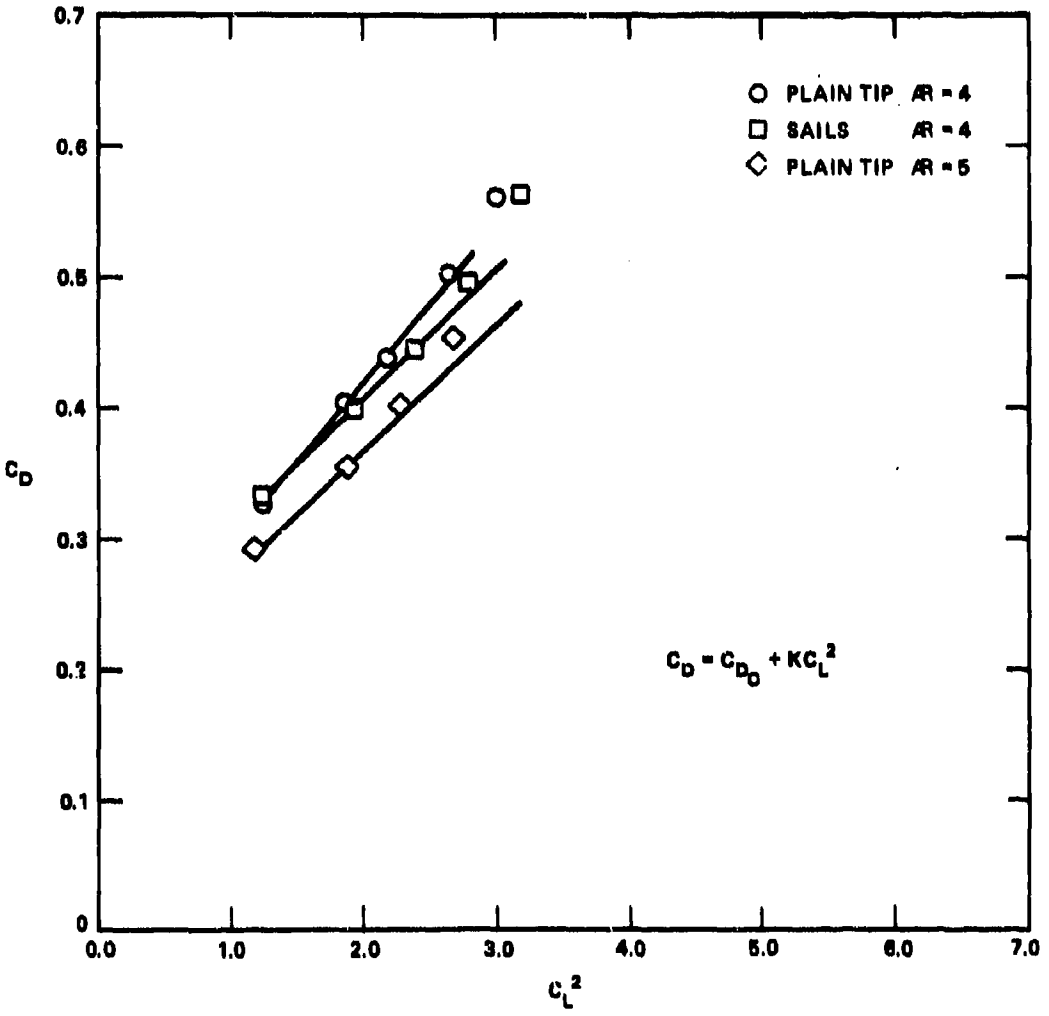

Figure 25 - Induced Drag Factor for USB Configuration, δ_f = 0 Degrees, δ_n = 0 Degrees

Figure 26 - Longitudinal Characteristics of CCW/USB Configuration, AR = 4, C_T = 0.6, δ_p = 40 Degrees

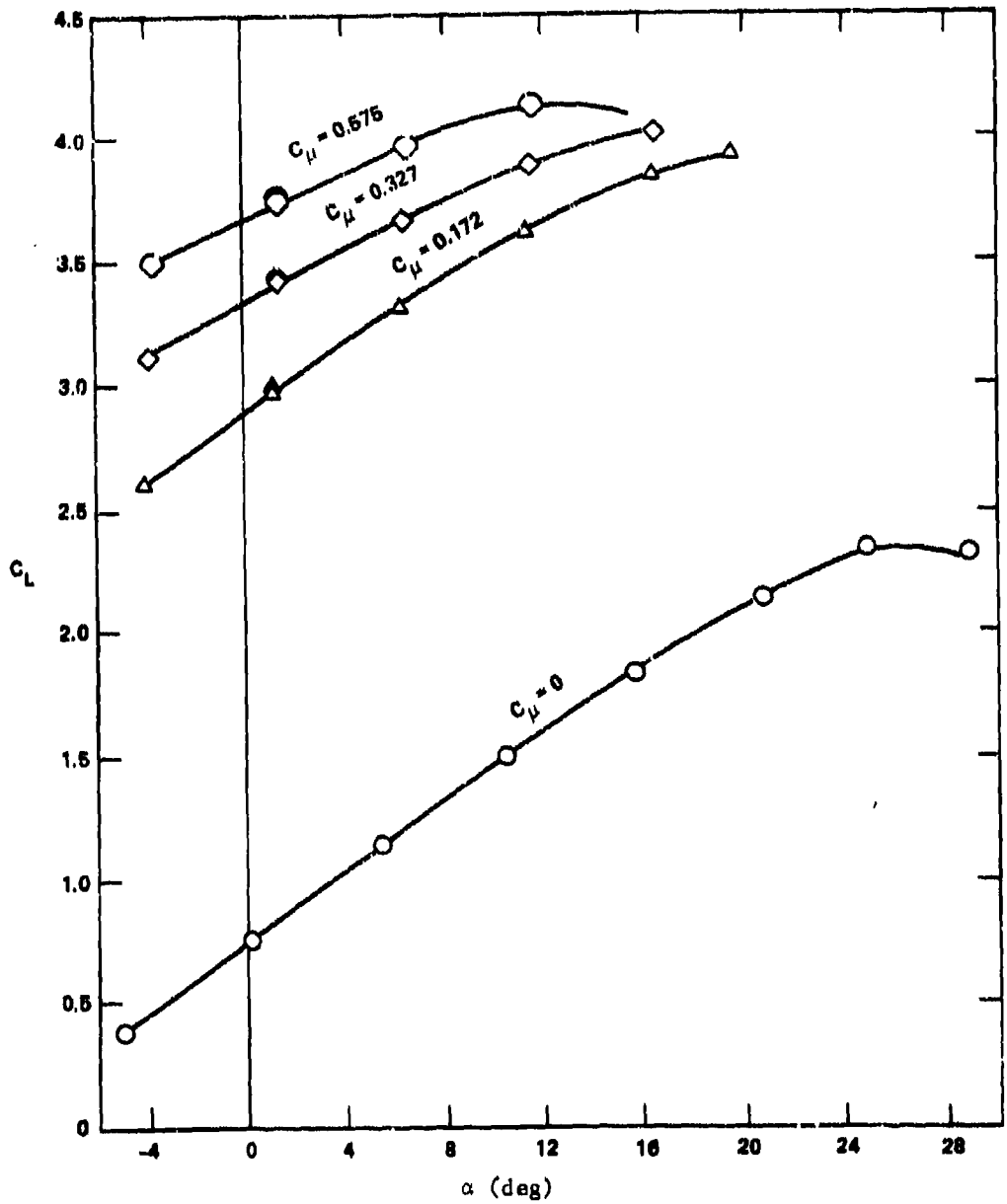

Figure 26a - Lift Curve

Figure 26 (Continued)

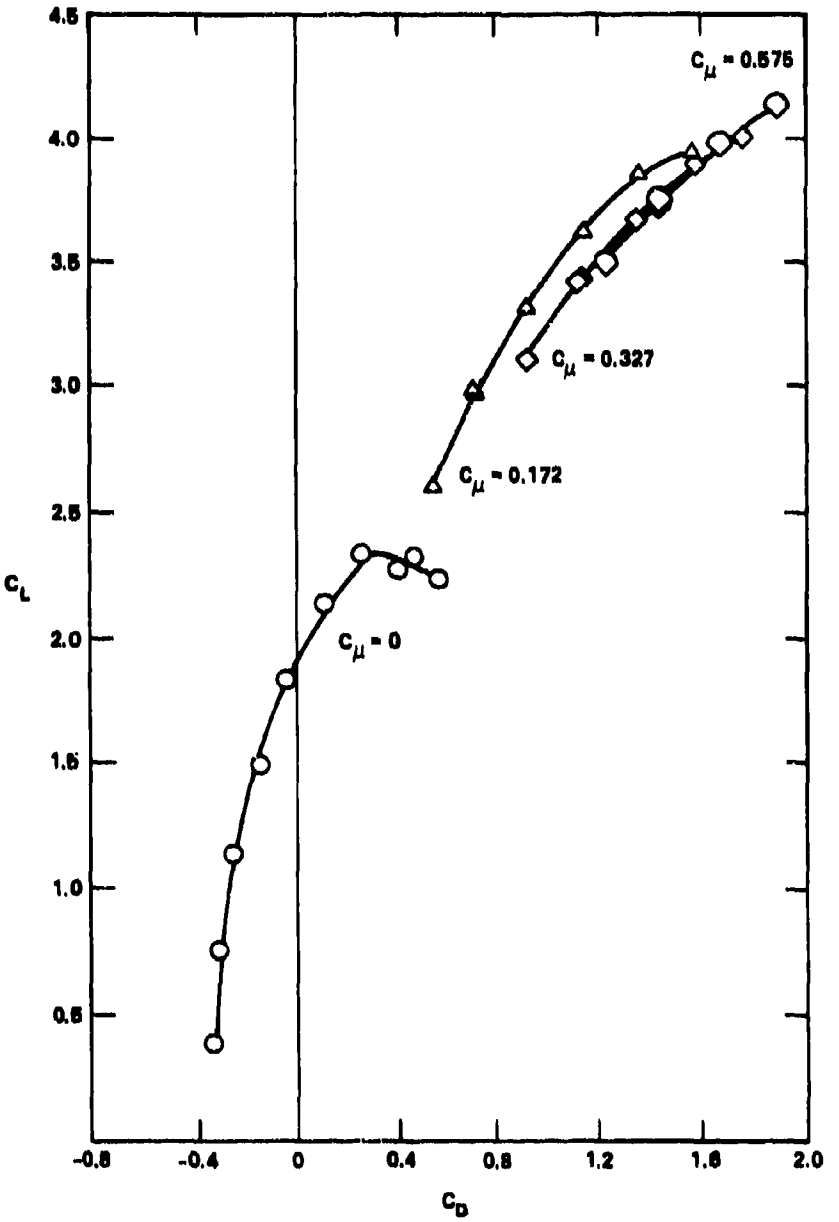

Figure 26b - Drag Polar

Figure 27 - Longitudinal Characteristics of CCW/USB Configuration, AR = 4, C_T = 1.19, δ_n = 40 Degrees

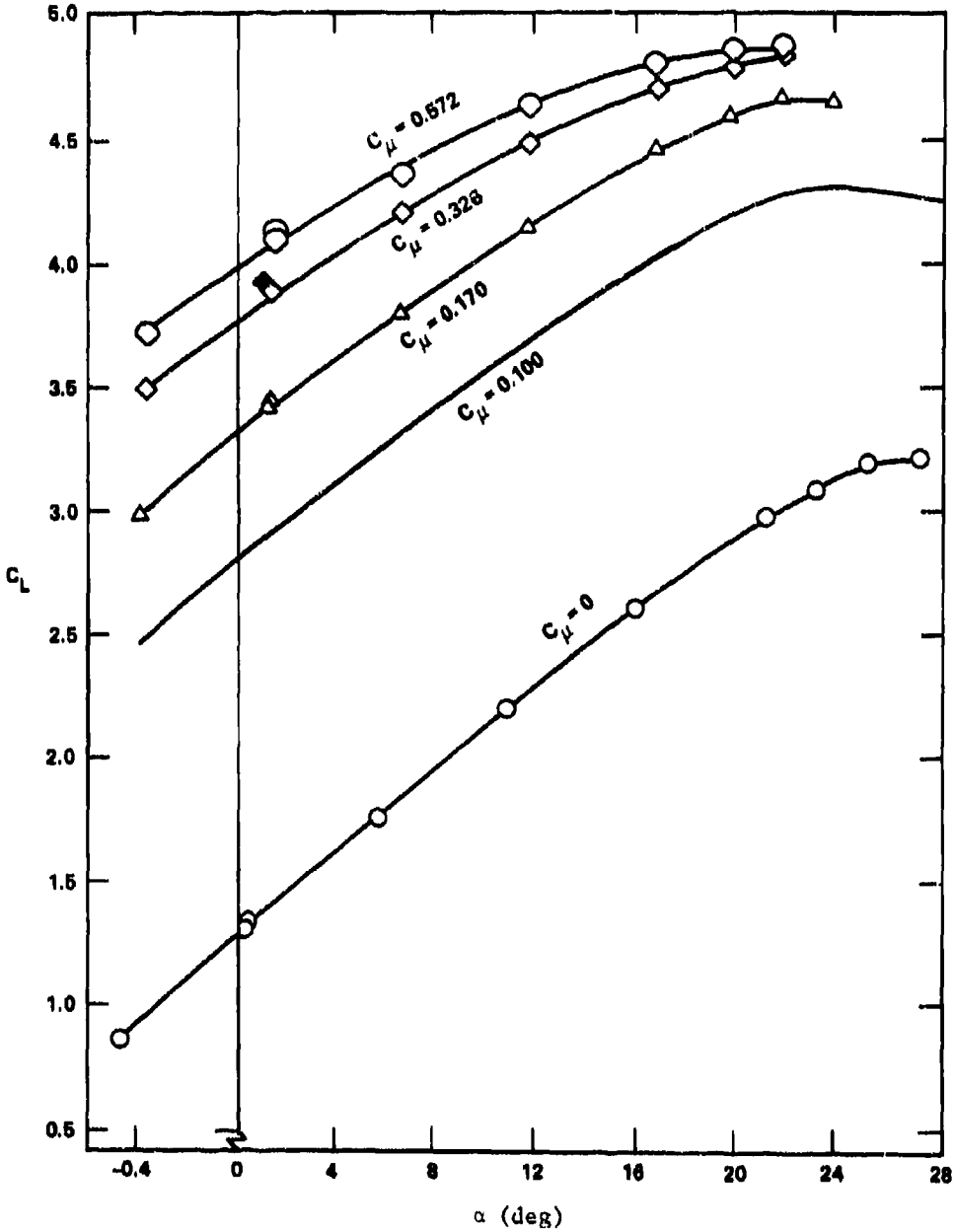

Figure 27a - Lift Curve

Figure 27 (Continued)

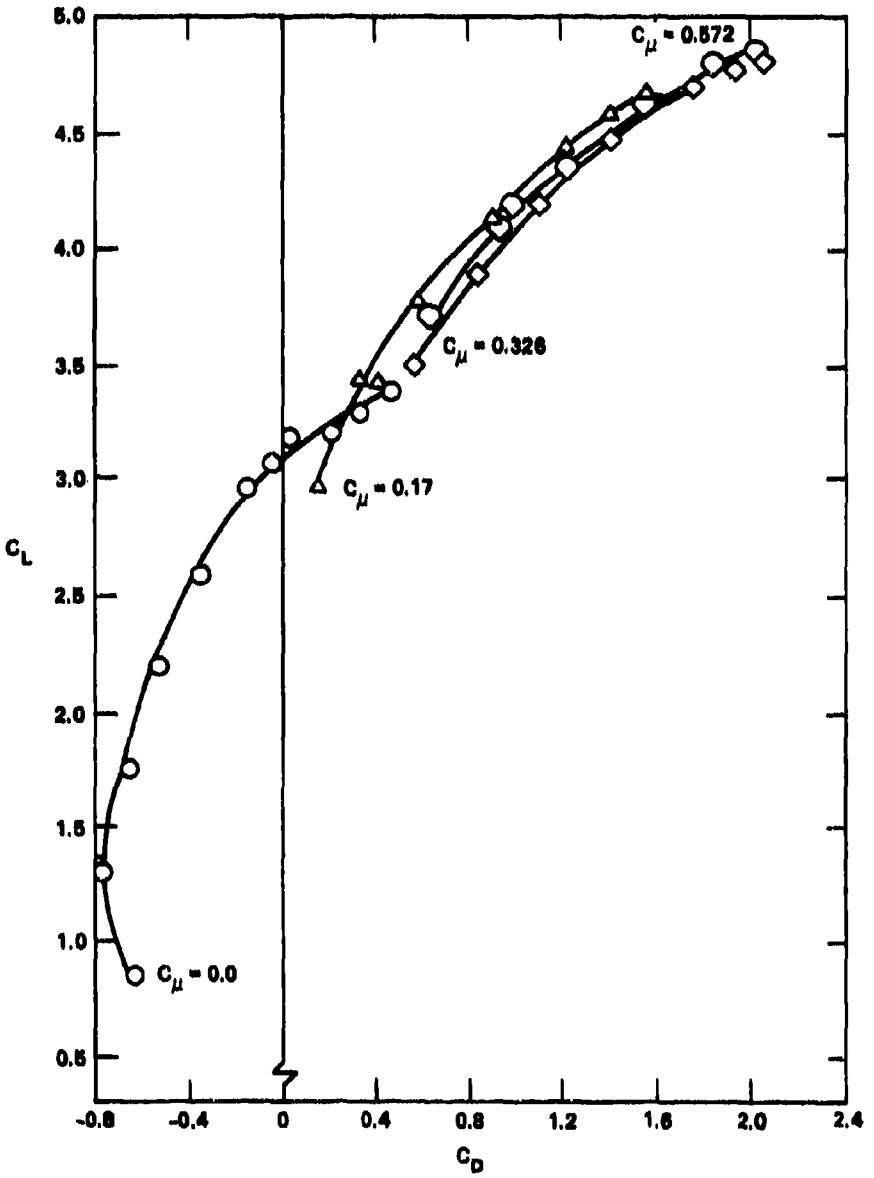

Figure 27b - Drag Polar

Figure 28 - Longitudinal Characteristics of CCW/USB Configuration, AR = 4, C_T = 1.45, δ_n = 40 Degrees

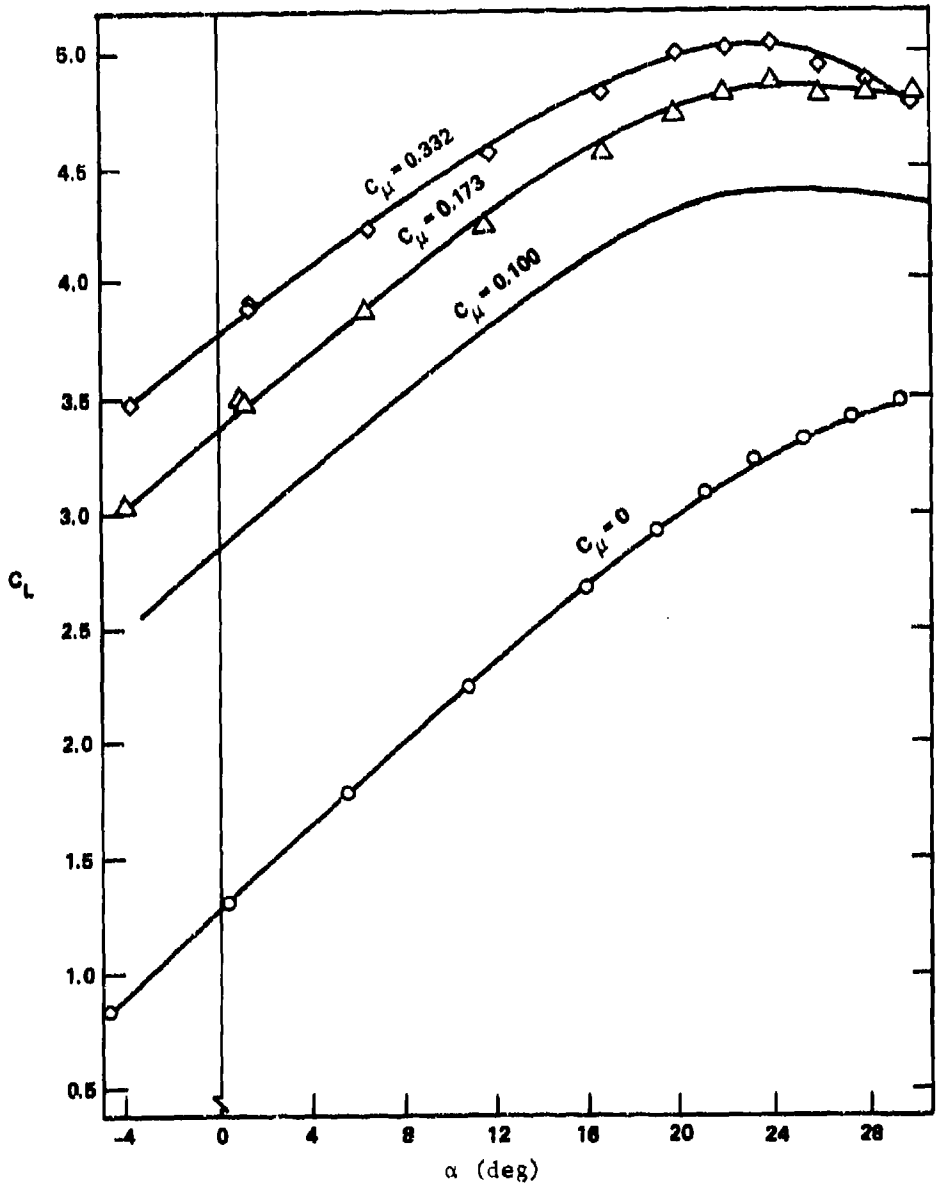

Figure 28a - Lift Curve

Figure 28 (Continued)

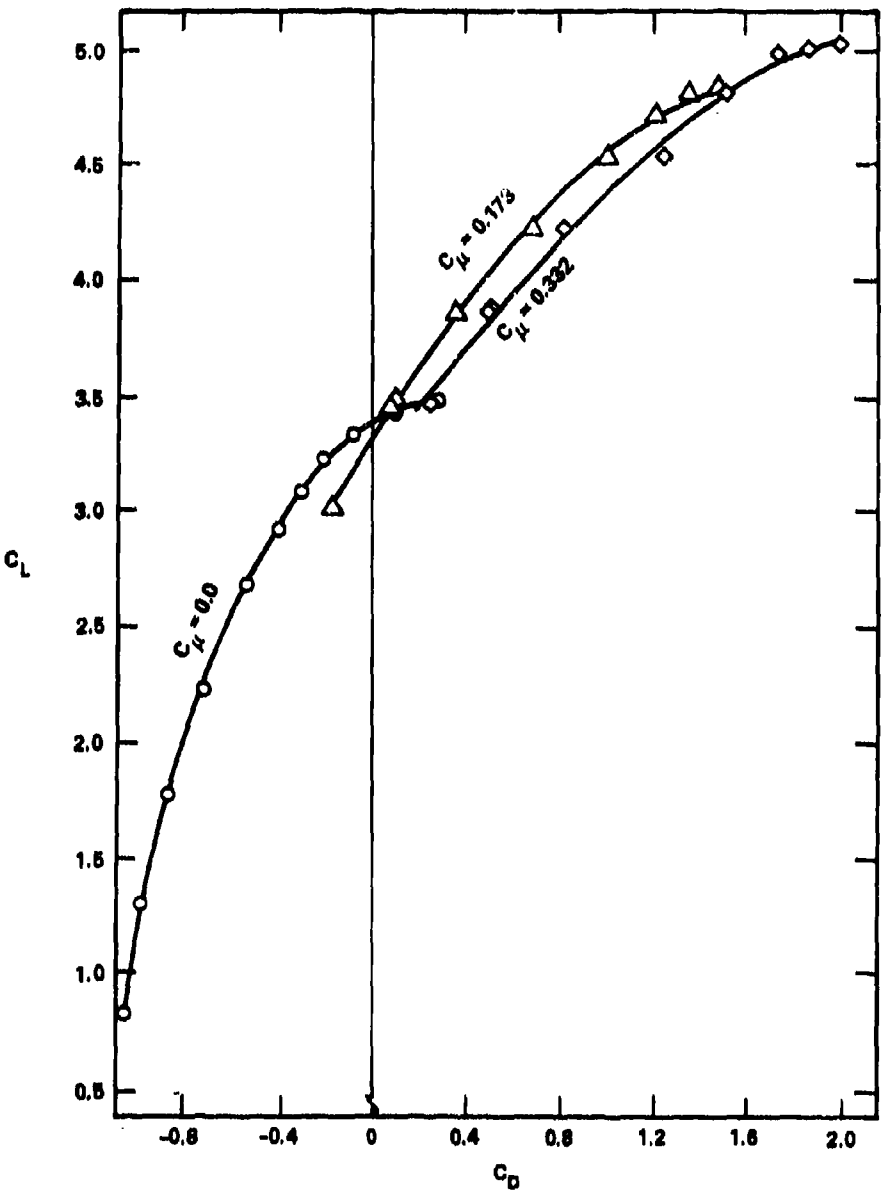

Figure 28b - Drag Polar

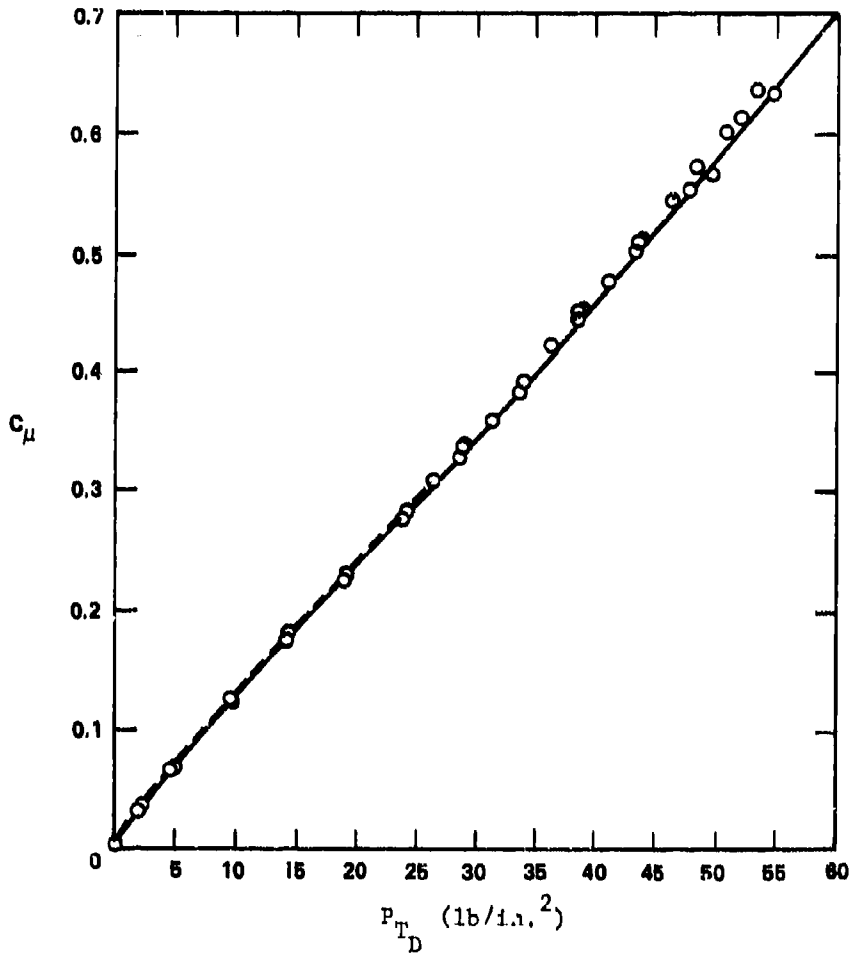

Figure 29 - Blowing Coefficient versus Duct Pressure for CCW/USB

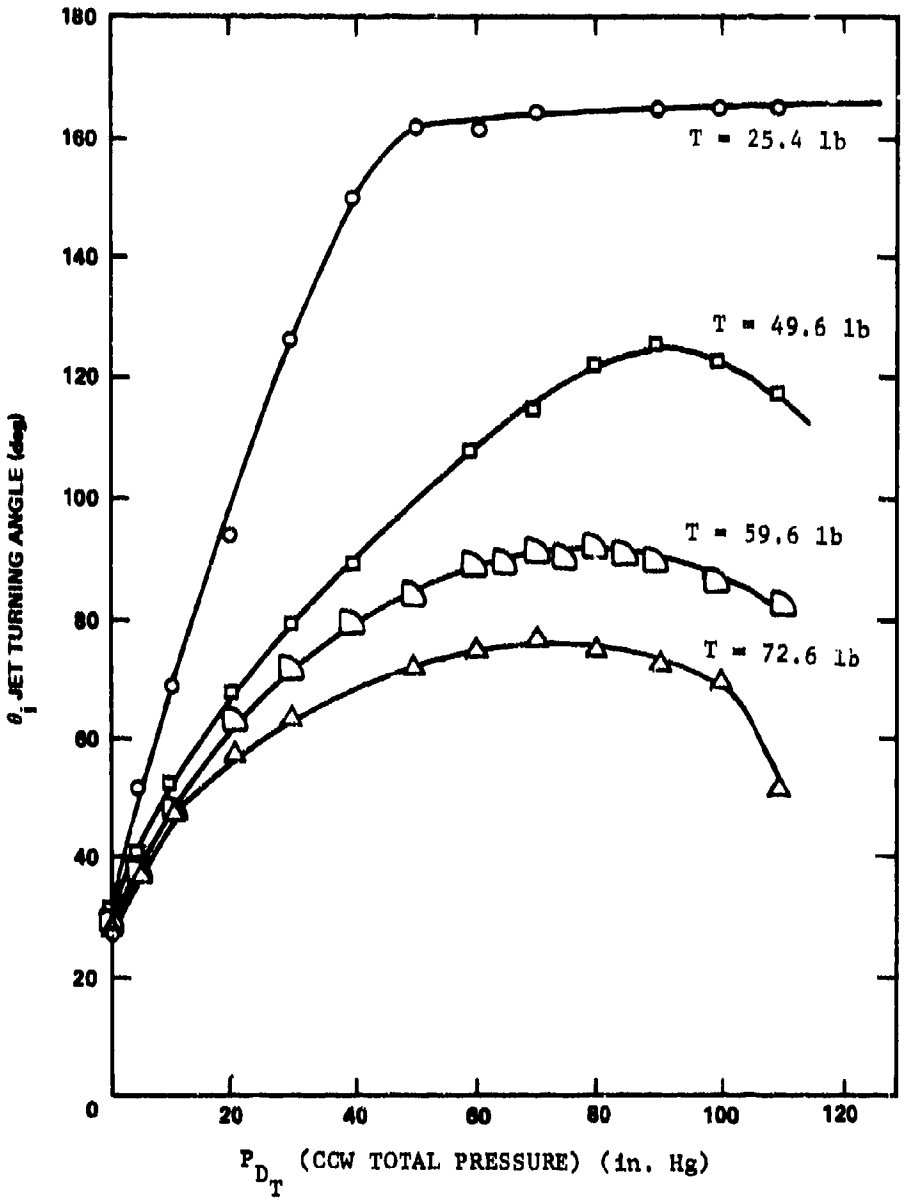

Figure 30 - CCW/USB Static Engine Thrust Turning

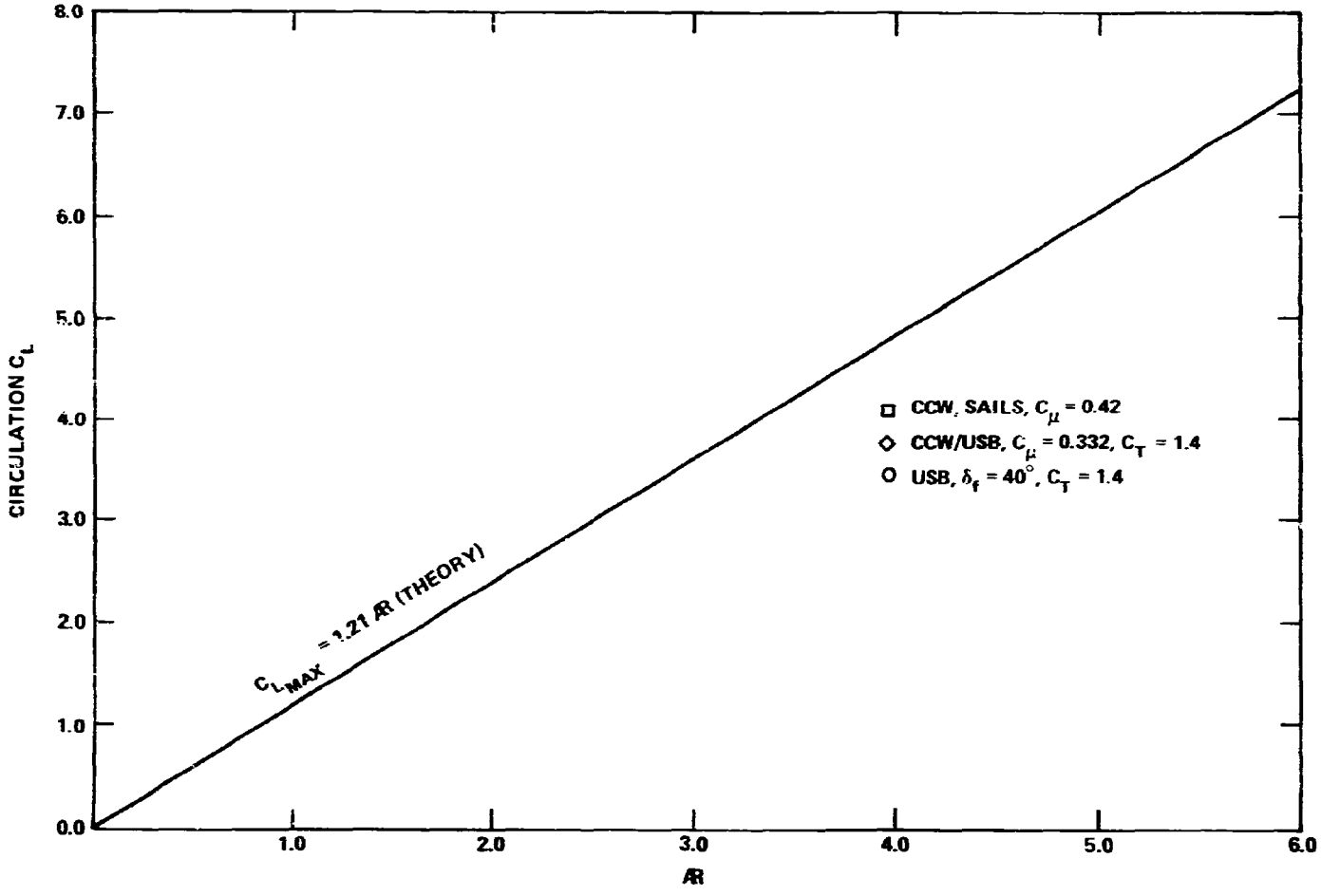

Figure 31 - Induced Circulation Lift

REFERENCES

1. Nichols, J.H., Jr., "Development of High Lift Devices for Application to Advanced Navy Aircraft," DTNRSDC-80/058 (Apr 1980); also presented at Workshop on V/STOL Aerodynamics, Naval Post Graduate School, Monterey, CA (16-18 May 1979).

2. Phelps, A.E., III, "Wind Tunnel Investigation of a Twin Engine Straight-Wing Upper-Surface Blown Jet-Flap Configuration," NASA TN D-7778 (Jan 1975).

3. Sleeman, W.C., Jr., and W.C. Hoklweg, "Low Speed Wind Tunnel Investigation of a Four-Engine Upper Surface Blown Model Having a Swept Wing and Rectangular and D-Shaped Exhaust Nozzles," NASA TN D8061 (Dec 1975).

4. Perry, B., III and G.C. Greene, "Wind-Tunnel Investigation of Aerodynamic Loads on a Large-Scale Externally Blown Flap Model and Comparison with Theory," NASA RN D-7863 (Mar 1975).

5. Woodrey, R.W., et al., "An Experimental Investigation of a Vectored Engine Over-Wing Powered Lift Concept," AFFDL-TR-76-92 (Sep 1976).

6. Englar, R.J. and R.A. Hemmerly, "Design of the Circulation Control Wing STOL Demonstrator Aircraft," Paper 79-1842 presented at AIAA Aircraft Systems and Technology Meeting, New York (20-22 Aug 1979).

7. Spillman, J.J. and J.E. Allen, "The Use of Wing Tip Sails to Reduce Vortex Drag," Cranfield Institute of Technology (Jun 1976).

8. McCormack, B.W., Jr., "Aerodynamic of V/STOL Flight," Academic Press, New York (1967), pp. 53-57.

DTNSRDC ISSUES THREE TYPES OF REPORTS

1. DTNSRDC REPORTS, A FORMAL SERIES, CONTAIN INFORMATION OF PERMANENT TECHNICAL VALUE. THEY CARRY A CONSECUTIVE NUMERICAL IDENTIFICATION REGARDLESS OF THEIR CLASSIFICATION OR THE ORIGINATING DEPARTMENT.

2. DEPARTMENTAL REPORTS, A SEMIFORMAL SERIES, CONTAIN INFORMATION OF A PRELIMINARY, TEMPORARY, OR PROPRIETARY NATURE OR OF LIMITED INTEREST OR SIGNIFICANCE. THEY CARRY A DEPARTMENTAL ALPHANUMERICAL IDENTIFICATION

3. TECHNICAL MEMORANDA, AN INFORMAL SERIES, CONTAIN TECHNICAL DOCUMENTATION OF LIMITED USE AND INTEREST. THEY ARE PRIMARILY WORKING PAPERS INTENDED FOR INTERNAL USE. THEY CARRY AN IDENTIFYING NUMBER WHICH INDICATES THEIR TYPE AND THE NUMERICAL CODE OF THE ORIGINATING DEPARTMENT. ANY DISTRIBUTION OUTSIDE DTNSRDC MUST BE APPROVED BY THE HEAD OF THE ORIGINATING DEPARTMENT ON A CASE-BY-CASE BASIS.